

# Abstract

Akbay, Mehmet Cuneyt. Performance of Compliant Electrodes in Electro Active Polymer (EAP) Actuators. (Under the direction of Dr. Tushar K. Ghosh and Dr. John F. Muth)

Dielectric elastomer (DE) actuators, based on the field-induced deformation of elastomeric polymers with compliant electrodes, can produce a large strain response. To accommodate the high strain during actuation the electrodes around the DE should also deform without imposing any restraints while maintaining their conductivity. The electrodes have to be compatible with the DE in their mechanical properties. In addition to mechanical properties such as elastic moduli, hysteresis, etc., other properties such as conductivity, percolation, are also of importance. Therefore the compliant electrode is a key feature of the DE actuator technology.

Many types of compliant electrodes used in conjunction with DE actuators have been reported in the literature. Among them are particle included polymers, metals, and conductive polymers. Particle included polymer based electrodes generally consist of carbon or silver as particles and a polymer medium such as silicone. Conductive polymers such as polypyrrole can be used as compliant electrode as well.

In this work an effort has been made to characterize various compliant electrodes on dielectric elastomer EAPs under different process conditions. Characterization of the electrodes includes their response to applied voltage, their conductivity values under different test conditions and their topography.

Three different types of compliant electrode have been characterized. These were rubber electrodes, grease electrodes and polypyrrole electrodes. The results showed that the crack formation was related with the amount of polymer carrier for

grease and rubber electrodes. Both rubber and grease electrodes, which were prepared with Nusil CF19-2186, showed the worst results in terms of uniformity of the electrodes and areal strain rates to the applied voltage. For rubber electrodes, electrodes, which were prepared with Sylgard 186 and Sylgard 184, showed similar results in terms of uniformity of the electrode. Generally Sylgard 184 rubber electrodes showed higher areal strain rates to the applied voltage than that of Sylgard 186 electrodes. Higher conductivity values were achieved with Sylgard 186 rubber electrodes comparing to Sylgard 184 rubber electrodes.

For grease electrodes, electrodes, which were prepared with Sylgard 186 and Sylgard 184 did not show similar results in terms of uniformity and areal strain. Higher conductivity values were observed with Sylgard 186 grease electrodes comparing to Sylgard 184 grease electrodes.

Both Sylgard 184 and Sylgard 186 rubber electrodes lost its conductivity at 100%-100% nominal strain rate.

It was observed that increasing the number of polymerizing process, thus number of rinsing, enable to remove black pyrrole particles more efficiently for polypyrrole electrodes. Relatively higher conductivity values and lower areal strain values were achieved with Ppy electrodes comparing to rubber and grease electrodes. Ppy electrodes lost its conductivity at 100%-100% nominal strain ratio.

# **Performance of Compliant Electrodes in Electro Active Polymer (EAP) Actuators**

**By**

**Mehmet Cuneyt Akbay**

**A thesis submitted to the Graduate Faculty of  
North Carolina State University  
in partial fulfillment of the  
requirements for the Degree of  
Master of Science**

**Textile Management and Technology**

**Raleigh, North Carolina**

**2004**

**Approved By:**

---

**Tushar K. Ghosh**  
Chair of Advisory Committee

---

**John F. Muth**  
Co-Chair of Advisory Committee

---

**Richard Kotek**  
Member of Advisory Comm

*Thanks GOD for giving me this opportunity.*

*I dedicate my thesis to my mother, my dad  
and my brother who are the most important  
and unique people in my  
life.....*

# Biography

Mehmet Cuneyt Akbay was born on November 1, 1971 and received his Bachelor of Science degree in Textile Engineering from Aegean University at Izmir, Turkey in 1993. He worked as a Texturizing Plant Chief at Insa A.S Istanbul-Turkey between November 1995 and June 2001 for six years prior to joining North Carolina State University for M.S. in Textile Management Technology.

# Acknowledgements

I would like to thank my chair of advisory committee, Dr. Tushar K. Ghosh for his support and guidance throughout this dissertation. I also would like to thank my co-chair of advisory committee Dr. John F. Muth and my committee member Dr. Richard Kotek. All my committee members have been a tremendous influence on my academic development during my research.

I am also grateful to the staff of College of Textiles, for all help and suggestions during my Masters.

I would like to thank my friends who shared my pains during my dissertation and project co-workers because of their supports and helps.

Finally I would like to thank my family. Without them I would not be here.

# Table of Contents

<b>LIST OF TABLES</b>	<b>VIII</b>
<b>LIST OF FIGURES</b>	<b>IX</b>
<b>1 INTRODUCTION.....</b>	<b>1</b>
<b>2 BACKGROUND.....</b>	<b>3</b>
2.1 ELECTRO ACTIVE POLYMERS (EAPs).....	4
2.1.1 Ionic EAPs.....	5
2.1.1.1 Ionic Polymer Gels (IPG).....	8
2.1.1.2 Ion-exchange Polymer-Metallic Composites (IPMC).....	9
2.1.1.3 Conductive Polymers (CP).....	9
2.1.1.4 Carbon Nanotubes (CNT).....	10
2.1.1.5 Electro Rheological Fluids (ERF).....	10
2.1.2 Electric EAPs.....	11
2.1.2.1 Ferroelectric Polymers.....	12
2.1.2.2 Dielectric Elastomer EAPs.....	13
2.1.2.3 Electrostrictive Graft Elastomers.....	14
2.1.2.4 Electrostrictive Paper.....	14
2.1.2.5 Electro-Viscoelastic Elastomers .....	15
2.1.2.6 Liquid Crystal Elastomer (LCE) Materials.....	15
2.2 DIELECTRIC ELASTOMER EAPs.....	15
2.2.1 Actuation Mechanism of DE EAPs.....	16

2.2.1.1 Maxwell Pressure.....	16
2.2.1.2 Dielectric Elastomers.....	17
2.3 COMPLIANT ELECTRODES.....	31
2.3.1 Grease and Rubber Electrodes.....	32
2.3.2 Conductive Polymer Electrodes.....	37
2.3.3 Metal Electrodes.....	44
<b>3 RESEARCH OBJECTIVE.....</b>	<b>50</b>
<b>4 EXPERIMENTAL.....</b>	<b>51</b>
4.1 MATERIALS .....	51
4.1.1 Grease and Rubber Electrodes.....	51
4.1.2 Polypyrrole Electrodes.....	51
4.1.3 Dielectric Elastomer.....	52
4.2 ACTUATOR FABRICATION.....	52
4.2.1 Preparation and Application of Electrodes.....	53
4.2.1.1 Rubber Electrodes.....	54
4.2.1.2 Grease Electrodes.....	56
4.2.1.3 Polypyrrole Electrodes.....	56
4.3 EVALUATION of ELECTRODES.....	59
4.3.1 Topography of Electrodes.....	59
4.3.2 Electrical Conductivity.....	60
4.3.2.1 Effect of Strain.....	63
4.3.3 Actuation Strain as a Function of Applied Voltage.....	64

<b>5 RESULTS and DISCUSSION.....</b>	<b>66</b>
5.1 TOPOGRAPHY of ELECTRODES. ....	66
5.1.1 Nusil CF19-2186 Grease and Rubber Electrodes.....	66
5.1.2 Sylgard 184 Grease and Rubber Electrodes.....	69
5.1.3 Sylgard 186 Grease and Rubber Electrodes.....	71
5.1.4 PPy Electrodes.....	74
5.2 CONDUCTIVITY of ELECTRODES.....	76
5.2.1 Sylgard 184 Rubber Electrodes.....	76
5.2.2 Sylgard 186 Rubber Electrodes.....	78
5.2.3 Sylgard 184 Grease Electrodes.....	80
5.2.4 Sylgard 186 Grease Electrodes.....	81
5.2.5 PPy Electrodes.....	82
5.2.6 Conductivity as a Function of Strain.....	83
5.2.6.1 PPy Electrodes.....	83
5.2.6.2 Sylgard 184 Rubber Electrodes.....	85
5.2.6.3 Sylgard 186 Rubber Electrodes.....	86
5.2.7 Percolation Threshold.....	88
5.3 ACTUATION STRAIN.....	89
5.3.1 Sylgard 184 .....	89
5.3.2 Sylgard 186 .....	91
5.3.3 Polypyrrole Electrodes .....	93
<b>6 CONCLUSION.....</b>	<b>94</b>
<b>7 REFERENCES.....</b>	<b>96</b>

# List of Tables

Table 1: Comparison of the properties of EAP, SMA and EAC [1].....	5
Table 2: Maximum response of representative elastomers [4].....	19
Table 3: Circular and linear test results for different types of elastomers [50].....	24
Table 4: Comparison of natural muscle and man made actuator technologies [9].....	25
Table 5: Comparison of natural muscle and man made actuator technologies [51] .....	31

# List of Figures

Figure 1: Ionic EAPs actuator operating principle [11].....	6
Figure 2: Ionic EAPs actuator operating principle [11].....	7
Figure 3: EAP actuators energy and bandwith comparison [2] .....	11
Figure 4: Dielectric polymer actuator operating.....	17
Figure 5: Experiment set-up the x and y directions are horizontal and vertical, respectively [44].....	20
Figure 6: Stress/force vs electric field/voltage curve for sample with 500% x 300% pre-strain [44].....	21
Figure 7: Force/voltage curve for the same sample at different strains in the length direction [44].....	22
Figure 8: Electrical breakdown strength of isotropically pre-strained acrylic tape [44] .....	23
Figure 9: Strain and stress of DE actuator compared to various natural data points [9].....	26
Figure 10: Power density and work-per cycle for DE actuator compared to natural muscle data points [9] .....	27
Figure 11: Schematic design of the actuators [51].....	28
Figure 12: Picture of the acrylic dielectric elastomer actuator. The black arrow indicates the length changes that were imposed on the actuator by the muscle lever. [51].....	28
Figure 13: Maximal isometric contractions of the tested actuators [51] .....	29
Figure 14: Passive workloops of the tested actuators at an oscillatory frequency of 2Hz [51] .....	30
Figure 15: Active workloops of the tested actuators at an oscillatory frequency of 2Hz [51] .....	31
Figure 16: Schematic diagram for the testing of the electrode resistance [54] .....	34
Figure 17: Electrode resistance versus strain [54].....	34
Figure 18: Percolation experiment graphs for Sylgard 184 with different percentages [53] .....	36
Figure 19: Frame for drawing the PUE film [58].....	40
Figure 20: Resistance of the PPy electrode under elongation. The electrodes were prepared a) undrawn, b) 9.8% drawn, c) 17.9% drawn, d) 28.2% drawn, e) 35.3% drawn PUE films [58].....	41
Figure 21: Field induced displacement of the PUE films with PPy electrodes of various thickness [58] .....	42
Figure 22: Field induced displacement of the PUE films with a) the wrinkled PPy electrode and b) the unwrinkled one. The wrinkled electrode was prepared on the 10.5% drawn PUE film [58] .....	43
Figure 23: Field induced displacement of a) the doped PUE film with the wrinkled PPy electrode prepared on the 9.9% drawn PUE film, b) the doped PUE film with the unwrinkled PPy electrode and c) an undoped PUE film with a conventional gold electrode [58] .....	44
Figure 24: Zig-zag cold electrodes [4].....	45
Figure 25: Structured electrodes [4] .....	46
Figure 26:Optical microscope picture of the cross-section of a moule [49] .....	47
Figure 27: Schematic of an elastomer actuator/sensor [49].....	47

Figure 28: Photographs of gold sputtered electrodes [39] .....	48
Figure 29: Photographs of evaporation-deposited electrodes [39].....	49
Figure 30: Air gun.....	55
Figure 31: a) Film with mask b) Final actuator .....	56
Figure 32: Preparation of polymerizing pyrrole solution .....	57
Figure 33 Polypyrrole coated acrylic film.....	59
Figure 34:Olympus BX 60 .....	60
Figure 35: Sony/Tektronik 370 Programmable Curve Tracer .....	61
Figure 36: Microscope platform with arm and plastic plate .....	62
Figure 37: Conductivity measurement spots for electrodes .....	63
Figure 38:Frame on the lab-jack .....	64
Figure 39: PPy actuator (connected to the voltage supplier with alligator clamps).....	65
Figure 40: Nusil CF19-2186 grease electrode a) 10% graphite b) 20% graphite .....	67
Figure 41: Nusil CF19-2186 rubber electrode a) 5% graphite b) 10% graphite c) 20% graphite.....	68
Figure 42: Sylgard 184- Fluid 200® FL 50 CST grease electrode a) 5% graphite b) 10% graphite.....	69
Figure 43: Sylgard 184- Fluid 200® FL 50 CST grease electrodes a) 5% graphite b) 6% graphite c) 7% graphite d) 8% graphite e) 9% graphite f) 10% graphite .....	70
Figure 44: Sylgard 184- Fluid 200® FL 50 CST rubber electrode a) 5% graphite b) 10% graphite c) 20% graphite.....	71
Figure 45: Sylgard 186- Fluid 200® FL 50 CST grease electrode a) 5% graphite b) 10% graphite c) 20% graphite.....	73
Figure 46: Sylgard 186- Fluid 200® FL 50 CST rubber electrode a) 5% graphite b) 10% graphite c) 20% graphite.....	74
Figure 47: PPy electrode a) polymerized 3 times b) polymerized 5 times c) polymerized 10 times .....	75
Figure 48: Resistance values of 5, 10 and 20% Sylgard 184 rubber electrode as a function of distance between the probes.....	77
Figure 49: Comparison of the resistance values of the 5, 10 and 20% Sylgard 184 rubber electrodes .....	78
Figure 50: Resistance values of 5, 10 and 20% Sylgard 186 rubber electrode as a function of distance between the probes.....	79
Figure 51: Comparison of the resistance values of the 5, 10 and 20% Sylgard 186 rubber electrodes .....	79
Figure 52: Resistance values of 5 and 10% Sylgard 184 grease electrode as a function of distance between the probes.....	80
Figure 53: Resistance values of , 5, 10 and 20% Sylgard 186 grease electrode as a function of distance between the probes.....	81
Figure 54:Resistance values of PPy electrode with 3 different polymerizing layers (3,5 and 10 times as a function of probe distance.....	82
Figure 55:Resistance values of PPy electrode under 0%-0% and 50%-50% nominal strain	84
Figure 56: PPy electrode a) under 0%-0% nominal strain b) under 100%-100%nominal strain.....	84

Figure 57: Resistance values of Sylgard 184 10% rubber electrode under 0%-0% and 50%-50% nominal strain .....	85
Figure 58: Sylgard 184 10% rubber electrode a) under 0%-0% nominal strain b) under 100%-100%nominal strain.....	86
Figure 59: Resistance values of Sylgard 184 10% rubber electrode under 0%-0% and 50%-50% nominal strain .....	87
Figure 60: Sylgard 186 10% rubber electrode a) under 0%-0% nominal strain b) under 100%-100%nominal strain.....	87
Figure 61:Percolation experiments graph .....	89
Figure 62: Applied voltage-strain curve for Slygard 184- Fluid 200® FL 50 CST grease electrodes .....	90
Figure 63: Applied voltage-strain curve for Sylgard 184- Fluid 200® FL 50 CST rubber electrodes .....	91
Figure 64: Applied voltage-strain curve for Sylgard 186- Fluid 200® FL 50 CST grease electrodes .....	92
Figure 65: Applied voltage-strain curve for Sylgard 186- Fluid 200® FL 50 CST 5% rubber electrode .....	92
Figure 66: Applied voltage-strain curve for PPy electrode.....	93

# 1 Introduction

Natural muscles are considered as ideal actuators because of their high energy density, fast speed of response, and large stroke length. All of these characteristics are desirable in many applications. Research efforts are underway for a long time to develop "artificial muscle actuators for robotic applications.

During the recent years, a new class of polymers is being investigated for their response to electrical stimulation with a significant shape or size change. These polymers have been described as Electro Active Polymers (EAPs). This potential of the EAPs is very important for engineers and scientists from many different disciplines. The most important characteristic is their similarity to biological muscles and their ability to induce large displacements [1].

EAPs can be formulated to have a wide range of electronic and/or electro-optical properties that can be tailored through the chemical composition and structure of the polymers themselves. These properties can often be made to change in response to external stimuli such as applied electric or magnetic field, light, pH and stress [2].

According to their actuation mechanism EAPs can be broadly divided into two categories [3];

1. Ionic EAPs
2. Electric EAPs

The distinction between these two groups will be discussed further in sections 2.1.1 and 2.1.2

One of the subgroups of Electric EAPs is Dielectric (DE) EAPs. These materials are also known as electrostatically stricted polymers (ESSP). Electrostatically stricted polymers are the materials that contain a flexible backbone polymer and grafted crystalline groups and offer high strain under an applied electric field. These polymers characterized by low elastic stiffness and high dielectric constant can be used to induce large actuation strain by subjecting them to an electrostatic field.

The working principle of Dielectric Elastomers (DE) is most easily understood when comparing them to a capacitor. They consist of a thin film between two electrodes. The actuation of dielectric EAPs is due to Maxwell Stress, discussed in further detail in section 2.2.1.1 [1].

The choice of materials and fabrication of the electrode for dielectric EAPs is an ongoing area of research. Among the electrode properties that are relevant to actuator performance is its ability to deform. If the electrodes cannot stretch in at least one planar direction of the dielectric film, actuation will be dramatically reduced. Because of this, compliant electrodes are the key feature of the Electro Active Artificial Muscle (EPAM) technology. Compliant electrodes will be discussed in section 2.3 [4].

There are two limits of actuation for a dielectric actuator; these are dielectric failure (breakdown) and loss of conductivity of the electrodes under strain. An ideal conformable electrode should allow actuation up to dielectric failure of the dielectric actuator. Therefore, in order to determine the compliant electrode performance evaluation of electrode conductivity as a function of strain and also actuation strain of the dielectric actuator as a function of applied voltage are important.

## 2. Background

The observation of electroactive behavior of polymers can be traced back to an 1880 experiment conducted by Roentgen. Roentgen used a rubber band with fixed end and a mass attached to the free end, and then he charged and discharged the rubber band. Another scientist Sacerdote followed this experiment with a formulation of the strain response to electric field activation in 1899. In 1925 scientists discovered the piezoelectric polymer. A piezoelectric polymer is defined as a material that changes shape when a voltage is applied to it, or releases a voltage when its shape is changed. There are many polymers that display volume or shape change in response to perturbation of the balance between repulsive intermolecular forces, which act to expand the polymer network and attractive forces to act to shrink it. Generally, electrical excitation is only one type of stimulator that can induce elastic deformation in polymers. Many polymeric materials can also be activated using chemical, thermal pneumatic, optical and magnetic stimulant as well [1, 5, 6].

Polymers that are chemically stimulated were discovered more than half a century ago when collagen filaments were demonstrated to reversibly contract or expand when dipped in acidic or alkali aqueous solutions, respectively. After observation of piezoelectric activity in poly (vinylidene fluoride), investigators started to examine other polymer systems, and a series of effective materials have emerged. The largest progress in EAP materials development has occurred in the last ten years where effective materials that can induce strains exceeding 100% have emerged [5].

## **2.1. Electroactive Polymers (EAPs)**

As mentioned earlier, electroactive polymers are those that respond to electrical stimulation with a significant change in shape or size. The most important characteristic is their similarity to biological muscles and their ability to induce large displacements [2, 4, 5, 7, 8].

Before EAPs, electroactive ceramics [EAC] and shape memory alloys [SMA] have been the primary source of actuation materials for smart structures and actuation mechanisms for many years. Application of these materials includes robotics, active damping, vibration isolation, manipulation, articulation, and many others. On the other hand, EAPs received relatively little attention due to the small number of available materials, and their limited actuation capability [1, 5, 8].

During the last ten years many new and effective EAP materials have been identified and improved fabrication techniques have emerged that have demonstrated potential capabilities of these materials. Table 1 shows the comparison of some of the relevant properties of EAP, SMA and EAC [5, 9, 10].

*Table 1: Comparison of the properties of EAP, SMA and EAC [1]*

Property	Electroactive polymers (EAP)	Shape memory alloys (SMA)	Electroactive Ceramics (EAC)
Actuation strain	>10%	<8% short fatigue life	0.1 - 0.3 %
Force (MPa)	0.1 - 3	about 700	30-40
Reaction speed	μsec to sec	sec to min	μsec to sec
Density	1- 2.5 g/cc	5 - 6 g/cc	6-8 g/cc
Drive voltage	2-7V/10-100V/μm	NA	50 - 800 V
Consumed Power	m-watts	Watts	watts
Fracture toughness	resilient, elastic	Elastic	fragile

As seen Table 1, EAPs can induce strains that are as high as two orders of magnitude greater than the striction-limited, EACs. Also EAPs are superior to SMAs in higher response speed, lower density, and greater resilience. So generally EAPs hold a great deal of potential [1, 3, 10].

The EAPs are classified into two categories based on their mechanism of actuation, ionic and electric [1];

### *2.1.1 Ionic EAPs*

Polymers containing ions have been referred to as ionic polymers. An ionic polymer is a material that contains a loosely collected arrangement of charged atoms (ions) bonded to the molecular 'backbone'.

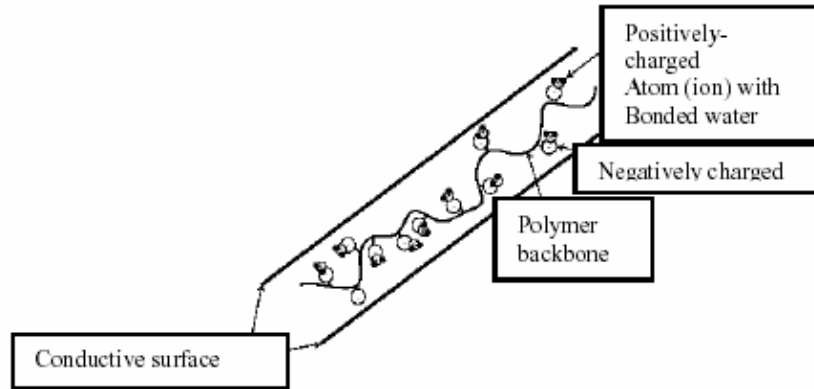
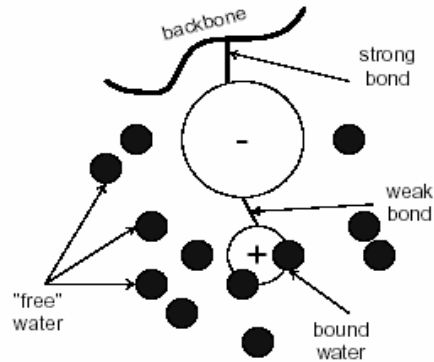


*Figure 1: Ionic EAPs actuator operating principle [11]*

In the early 1990s, it was demonstrated that applying a voltage across an ionic polymer produces mechanical deformation. Conversely, application of mechanical deformation produces charge flow. These materials show change in shape or dimension due to migration of electrons in response to electric field [1, 2, 5, 11]. Thus, ionic materials can be used as electromechanical sensors and actuators. The key to understanding this behavior is related to the strength of the bonds between those negatively charged side groups and the positively charged ions. When the material is hydrated, the bond between the positive ions (cations) and the negative side group weakens while the side group maintains a strong bond to the polymer backbone [11, 12, 13].



**The bond between the cation and the water remains strong.**

*Figure 2: Ionic EAPs actuator operating principle [11]*

On application of an electric field the weak bond between the cation and the side group breaks, freeing the cation to “move” in the polymer. The side group remains fixed to the backbone and doesn’t move. The motion of the cations also ‘drags’ water to the negatively charged surface. The motion of water produces a pressure gradient in the material. The result of the water motion is a pressure gradient through the thickness of the polymer. The pressure gradient produces a bending moment of on the material, resulting in mechanical strain and bending of the polymer [11].

Ionic EAPs can be classified into five groups according to their chemical properties [3];

1. Ionic Polymer Gels (IPG)
2. Ionomeric Polymer-Metal Composites (IPMC)
3. Conductive Polymers (CP)
4. Carbon Nanotubes (CNT)
5. ElectroRheological Fluids (ERF)

### 2.1.1.1 Ionic Polymer Gels (IPG):

Polymer gels are multi-phase materials consisting of a cross-linked polymer network and interstitial fluid. They are cross-linked polymers swollen in a solvent. The principle of the gel's motion is based on the molecular assembly reaction of cationic surfactant molecules with negatively charged hydrogel caused by both electrostatic and hydrophobic interactions to give the effective contraction. Generally, the swelling of ionic gel is attributed to the difference of osmotic pressure concerned with the freely mobile ions between inside and outside the gel. The contraction of the surfactant solution is connected with the neutralization of negative charges in the gel by forming with cationic surfactant molecules. Another factor affecting the volume of the gel is the interaction of the polymer and the interstitial fluid. The affinity between the polymer and fluid enables the polymer network to absorb the fluid and swell. The forces, which affect this interaction, work to increase the volume of the gel. Many different polymer gels have been developed which react to various kinds of environmental change such as pH change and the application of an electric field [14, 15].

Ionic polymer gels have the potential of matching the energy density and the force of biological muscles. One of the examples for these gels is polyacrylonitrile (PAC). The polyacrylonitrile materials are activated by chemical reaction(s), a change from an acid to an alkaline environment inducing an actuation through the gel becoming dense or swollen. Because of the diffusion of ions through the multilayered gel, the actuation of these materials is slow [16, 17].

### 2.1.1.2 Ion-exchange Polymer-Metallic Composites (IPMC)

A typical IPMC consists of a thin polymer membrane with metal electrodes plated on the both faces. IPMCs respond to an electrical activation as a result of the mobility of cations in the polymer network. The stimulation of an IPMC in the hydrated state results in a fast bending deformation. Both the fixed anions and the mobile counter-ions are subjected to an electric field because of the external stimulation and counter-ions become able to diffuse toward one of the electrodes. As a result, the composite undergoes a bending deformation toward the anode, followed by a slow relaxation in the opposite direction [1, 18, 19].

Generally, two types of base polymers are employed to form IPMCs these are Nafion<sup>®</sup> (perfluorosulphonate manufactured by Du Pont) and Flemion<sup>®</sup> (perfluorocoboxylate manufactured by Asahi Glass, Japan). IPMC require relatively low voltages to stimulate a bending response (1-10 V) with low frequencies below 1 Hz [16, 20].

### 2.1.1.3 Conductive Polymers (CP)

CPs are a class of materials that feature a conjugated backbone structure. These polymers exhibit chemically and electrochemically controllable electronic conductivities. CPs response to an electrical activation via the reversible counter-ion insertion and expulsion, that occurs during redox cycling. Significant volume changes occur through oxidation and reduction reactions at corresponding electrodes through exchanges of ions with an electrolyte [17, 21, 22].

Polypyrrole (PPy) and polyaniline are the two common conductive polymers that belong to this class. CP actuators require voltages in the range of 1-5 V. Variations to the voltage can control actuation speeds [17, 22, 23, 24].

#### 2.1.1.4 Carbon Nanotubes (CNT)

Carbon nanotubes are unique nanostructures. They have remarkable electronic and mechanical properties. Researchers have first focused on their exotic electronic properties, since nanotubes can be considered as prototypes for a one-dimensional quantum wire [25].

An ideal nanotube can be thought of as a hexagonal network of carbon atoms that has been rolled up to make a seamless cylinder. Just a nanometer across, the cylinder can be tens of microns long, and each end is "capped" with half of a fullerene molecule. Single-wall nanotubes can be thought of as the fundamental cylindrical structure, and these form the building blocks of both multi-wall nanotubes and the ordered arrays of single-wall nanotubes called ropes [25, 26].

The actuation mechanism of CNTs is through an electrolyte medium and the change in bond length via the injection of charges that affect the ionic charge balance between the nano-tube and the electrolyte. If more charges are injected into the CNT the dimension change be larger [17].

As a consequence of the mechanical strength and modulus of single CNTs and the achievable actuator displacements, these EAPs can boast the highest work per cycle and generate much higher mechanical stresses than other forms of EAPs [17, 27].

#### 2.1.1.5 ElectroRheological Fluids (ERF)

ERFs are electroactive fluids that change their rheological properties, in the presence of an electric field. These fluids are made from suspensions of an insulating base fluid and particles on the order of one tenth to one hundred microns in size [28].

ERFs rapidly solidify or increase their viscosity dramatically, in response to an electric field due to the formation of particle chains that bridge the electrodes. These materials are made by suspending particles in a liquid whose dielectric constant or conductivity is mismatched in order to create dipolar particle interactions in the presence of an AC or a DC electric field [29].

### 2.1.2 Electric EAPs

Electric EAPs are the polymers that can be driven or activated by an electric field or Coulomb forces. The electronic polymers (electrostrictive, electrostatic, piezoelectric, and ferroelectric) can be made to hold the induced displacement under activation of a DC voltage, allowing them to be considered for robotic applications. Except for CP, ionic EAPs don't hold strain under DC voltage. Also, electric EAPs have a greater mechanical energy density (see Figure 3) and they can be operated in air with no major constraints [1, 5, 17].

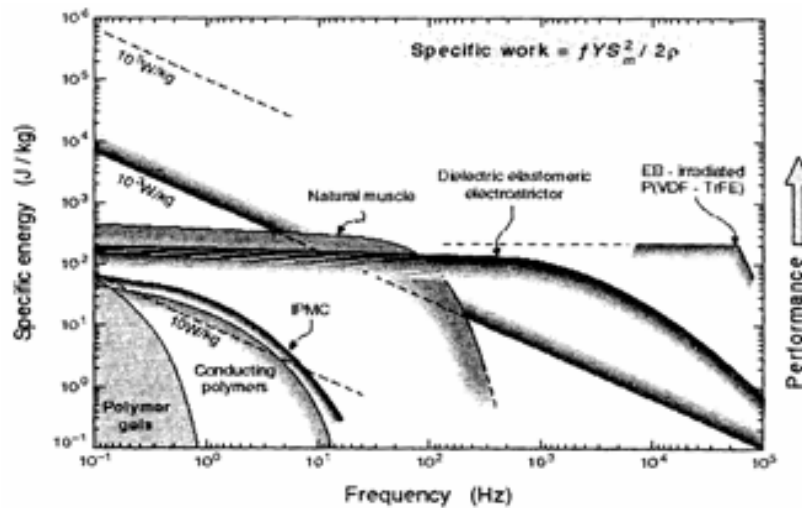


Figure 3: EAP actuators energy and bandwidth comparison [2]

Electric EAPs are very attractive in terms of energy conversion. This class of EAPs converts electric energy to mechanical energy and hence can be utilized as both solid-state electromechanical actuators and motion sensors. The electromechanical response in this class of polymers can be linear such as piezoelectric polymers or electrects or nonlinear such as the electrostrictive polymers and Maxwell stress effect induced response. Electric EAPs can require large electric fields ( $>100\text{-V/mm}$ ), to achieve longitudinal deformations at the range from 4-350% [13].

Electric EAPs can be classified into six groups according to their response to the applied electric field [3];

1. Ferroelectric Polymers
2. Dielectric Elastomers
3. Electrostrictive Graft Elastomers
4. Electrostrictive Paper
5. Electro-Viscoelastic Elastomers
6. Liquid Crystal Elastomer (LCE) Materials

#### 2.1.2.1 Ferroelectric Polymers

A ferroelectric polymer can be defined as a polymer in which the application of an electric field reverses the direction of spontaneous polarization. These kinds of polymers can be in a single crystal form or a semi-crystalline form in which the ferroelectric crystallites are embedded in an amorphous matrix. These polymers can be formed into thin flexible sheets [1, 30].

Poly (vinylidene difluoride) (PVDF) and its copolymers are the most promising materials of this class. Especially by electron irradiation treatment, very high strain and high energy density properties can be gained to these materials. Electric induced strain response in the copolymer is mainly from the electric field induced phase transition between nonpolar to polar phases in the crystalline area [29, 31, 32, 33].

Ferroelectric polymers have attracted a great deal of attention due to their many desirable properties, such as flexibility, light weight, high mechanical strength, ease of processability to large area films and ability to be molded into a desirable configuration. However they have some disadvantages. Most ferroelectric polymers have the disadvantages of low electric field sensitivity in terms of their dielectric constant, piezoelectric coefficient, electromechanical coupling coefficient, and field induced strain. These disadvantages limit their applications. PVDF and its copolymers are the most promising materials of this class [29, 34].

#### 2.1.2.2 Dielectric Elastomer EAPs

Dielectric elastomer EAPs are rubbery polymer materials that have a large electromechanical response to an applied electric field. Electrostatic fields can be applied to those polymers exhibiting low elastic stiffness and high dielectric constants to induce large actuation strain, these polymers are known as electro-statically stricted. Electrostriction is the property of the dielectrics that manifests as relatively slight change of shape or mechanical deformation under the application of an electric field. The actuation mechanism of dielectric EAPS is due to Maxwell stress. Dielectric EAP actuators require large electric fields ( $\sim 100 \text{ V}/\mu\text{m}$ ) and can produce large strain levels (10—350%) [1, 4, 8, 17, 29, 35, 36]. Dielectric elastomer EAPs will be discussed further in section 2.2.

### 2.1.2.3 Electrostrictive Graft Elastomers

A grafted elastomer is a material, which has a flexible polymer backbone and grafted crystalline groups. The grafted crystalline phase provides the polarizable moieties for the electric field response and serves as cross-linking sites for the elastomeric system. These elastomers offer large electric field induced strain [1, 37, 38].

In 1998, a graft elastomer EAP was developed at NASA Langley Research Center that exhibits a large electric field induced strain. The material exhibits high electric field induced strain (~4%) combined with mechanical power and excellent processability [34, 38].

### 2.1.2.4 Electrostrictive Paper

Electrostrictive papers produce large displacement with small force under an electrical excitation. Electrostrictive paper is a sheet that is composed of a multitude of discrete particles, mainly of a fibrous nature, which form a randomly organized network structure. These are produced in various mechanical processes with chemical additives. Because of this, it is possible to prepare a paper that has electroactive properties. The operational principle of electrostrictive paper is due to electrostriction effect associated with a combination of the electrostatic force of electrodes and the intermolecular interaction of the adhesives [39, 40, 41].

Kim et al investigated an electrostrictive paper actuator that has been prepared by bonding two silver laminated papers with silver electrodes placed on the outside surface. When an electric voltage is applied to the electrodes the actuator produces bending displacement, and its performance depends on the excitation voltages, frequencies, type of adhesive, and the host paper [39].

These types of actuators are lightweight, simple to fabricate and are likely to be used in applications such as active sound absorbers, flexible speakers and “smart” shape control devices [1].

#### 2.1.2.5 Electro-Viscoelastic Elastomers

Electro-viscoelastic materials are characterized as having stiffness and damping properties that vary with frequency, temperature and applied voltage. These materials are composites of silicone elastomers. After curing an electric field is applied that orientates the polar phase within the elastomeric matrix. An applied electric field ( $<6 \text{ V}/\mu\text{m}$ ) induces changes in shear modulus. Typical potential applications are as alternatives to electro-rheological fluids for active damping applications [29, 23].

#### 2.1.2.6 Liquid Crystal Elastomer (LCE) Materials

These materials possess EAP characteristics by inducing Joule heating. LCEs are composite materials consisting of monodomain nematic liquid crystal elastomers and conductive polymers, which are distributed within their network structure. The actuation mechanism is a phase transition between nematic and isotropic phases. The actuation takes place in less than a second [42, 43]

## **2.2 Dielectric Elastomer EAPs**

Polymers with low elastic modulus and high dielectric constant have been used to induce large actuation strain by subjecting the material to an electrostatic field. Dielectric EAP actuators require large electric fields ( $\sim 100 \text{ V}/\mu\text{m}$ ) and can produce strain levels 10%—350% [4, 8, 17, 29, 35, 44].

### *2.2.1 Actuation Mechanism of DE EAPs*

It has been well known that the electric field pressure from free charges on the surface of all insulating materials induces stresses that strain the material. This stress is called Maxwell stress. A dielectric elastomer actuator can be considered as a compliant capacitor where the polymer is sandwiched between two compliant electrodes. When a capacitor is charged, a pressure arises between the two electrodes. This pressure, known as the Maxwell pressure ( $p$ ), arises from the fact that the plus-charges on one electrode attract the minus-charges on the other, and the electrostatic forces resulting from the free charges squeeze and stretch the polymer. So dielectric elastomer technology function on the simple principle that, when a voltage is applied across the electrodes, the polymer shrinks in thickness direction and expands in its plane. These changes reduce the electrical energy and the difference is converted to mechanical work [1, 2, 4, 8, 9, 35, 36, 45, 46 ].

#### 2.2.1.1 Maxwell Pressure

As mentioned above, free charges, which are placed, on the surface of the insulating materials induces stresses when subjected to an electric field. These stresses strain the material and called Maxwell pressure. Maxwell pressure can produce powerful electroactive responses in certain elastomers [8, 46, 47, 48, 49, 50].

Maxwell pressure is created when a capacitor is charged. Electrostatic forces resulting from the free charges squeeze and stretch the polymer and as a result, the dielectric polymer as well as the electrodes expands in area. Stretching separates like charges and hence reduces electrical energy and also decreases the film thickness. The reduction in electrical energy is balanced by an increase in elastic mechanical energy and/or mechanical work output. Since the thickness of the film is decreased, electrodes come closer

to each other and in the process converts electrical energy to mechanical energy. For the compliant medium Maxwell pressure is expressed as;

$$p = \epsilon\epsilon_0 E^2 = \epsilon\epsilon_0 \left(\frac{V}{z}\right)^2$$

where E is the electric field,  $\epsilon$  is the dielectric constant,  $\epsilon_0$  is the permittivity of free space, V is the applied voltage and z is the polymer thickness [1, 4, 9, 45, 48]. Figure 4 shows the operation principle of dielectric polymer actuator.

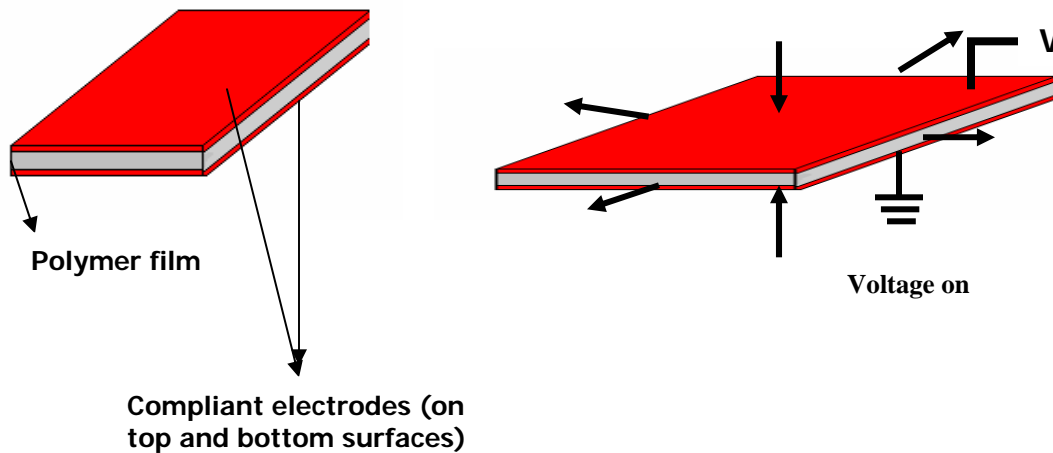


*Figure 4: Dielectric polymer actuator operating*

### 2.2.1.2 Dielectric Elastomers

As mentioned before dielectric elastomers are rubbery polymer materials that have a large electromechanical response to an applied electric field. These materials are also known as electrostatically stricted polymers. Important performance parameters for a

dielectric elastomer as an actuator are specific energy density, actuation pressure and strain, response time and efficiency. We can also add low viscoelastic losses, a wide range of temperature and humidity tolerance and ease of fabricating thin films to these properties [1, 4, 8, 17, 29, 35, 36]

We can characterize DE materials according to their two important mechanical properties. One is their ability to undergo large elastic strain and the other one is their ability to maintain volume during their deformation. Compared to many other electroactive materials such as piezoelectric ceramics and magnetostrictive ceramics, dielectric elastomers are relatively compliant, capable of extremely large strains and have high energy densities. These materials also have fast response time and high electromechanical efficiency. The technology is probably the most attractive polymer based actuator technology for robotic applications [44, 49].

Several dielectric elastomer polymers have shown good performance as an actuator. Silicones (based on poly(dimethyl siloxane)) and a commercial acrylic (available from 3M Corp.) have shown the greatest strain and total energy density. Maximum strains of more than 100% have been shown with both of these materials. The data in Table 2 identify the essential material performance of some of the relevant actuator materials [4]

Table 2: Maximum response of representative elastomers [4]

Polymer (Specific type)	Elastic Energy Density (J/cm <sup>3</sup> )	Pressure (MPa)	Strain (%)	Young's Modulus (MPa)	Electric Field (V/ $\mu$ m)	Dielectric Constant (@ 1 kHz)	Coupling Efficiency, $k^2$ (%)
Silicone Nusil CF19-2186	0.15	0.72	32	1.0	235	2.8	54
Silicone Dow Corning HS3 (centrifuged to remove particulates)	0.038	.13	41	0.125	72	2.8	65
Polyurethane Deerfield PT6100S	0.20	3.8	11	17	160	7.0	21
Silicone Dow Corning Sylgard 186	0.10	0.50	32	0.7	144	2.8	54
Fluorosilicone Dow Corning 730 (centrifuged to remove particulates)	0.051	0.29	28	0.5	80	6.9	48
Fluoroelastomer LaurenL143HC	0.016	0.39	8	2.5	32	12.7	15
Polybutadiene Aldrich PBD	0.025	0.41	12	1.7	76	4.0	22
Isoprene Natural Rubber Latex	0.010	0.19	11	0.85	67	2.7	21

Average engineering modulus at the maximum strain.

Kofod and his coworkers at SRI international [44], focused on understanding the basic physical mechanism underlying the observed electromechanical response of polyacrylate dielectric elastomers. They also considered factors affecting the dielectric strength of the material, since the maximum performance of an actuator will depend on the maximum electric field that can be applied to the material.

They used 3M 4910 VHB<sup>TM</sup> acrylic adhesive tape with carbon grease electrodes (from Circuit Works<sup>TM</sup>) in order to carry out their experiments. VHB 4910 is a very high bond structural adhesive from 3M. These tapes are available as a 1mm thick sheet, mounted on a red plastic liner, which makes it very easy to cut to preferred dimension. Due to its stickiness it is very easy to stretch and mount on frames, making it a very good material for testing demonstration devices. The film is translucent and extremely compliant and can be stretched easily in both directions in the plane of the film [39, 44].

Kofod et al [44] reported evaluation of stress/force as a function of electric field strength for VHB 4910 dielectric elastomer at different levels of pre-strains. The geometry of the set up that Kofod et. al. set for measuring the field induced stress is shown in Figure 5. The film was pre-strained 500% in the x direction and was glued to the plastic beams as shown in Figure 5. One of the beams was fixed to a translation table and the other was attached to a load cell. Conductive grease electrode was smeared on both sides of the film. Three different pre-strain levels in the y direction, 300%, 400% and 500% were used. The pre-strain in the y direction was controlled by a micrometer-screw. The load cell was zeroed at the specified pre-strain levels. On application of voltage (upto 5 kV), the recorded force-voltage curves were parabolic with an apparent relative dielectric constant of approximately 4. As shown at Figure6, the dotted lines are the expected parabolic curves corresponding to the relative dielectric constant written next to the curve. The experimental curve followed a parabolic behavior with an apparent relative dielectric constant 4. Figure 6 shows the stress/force vs electric field/voltage curve for sample with 500% x 300% pre-strain [44].

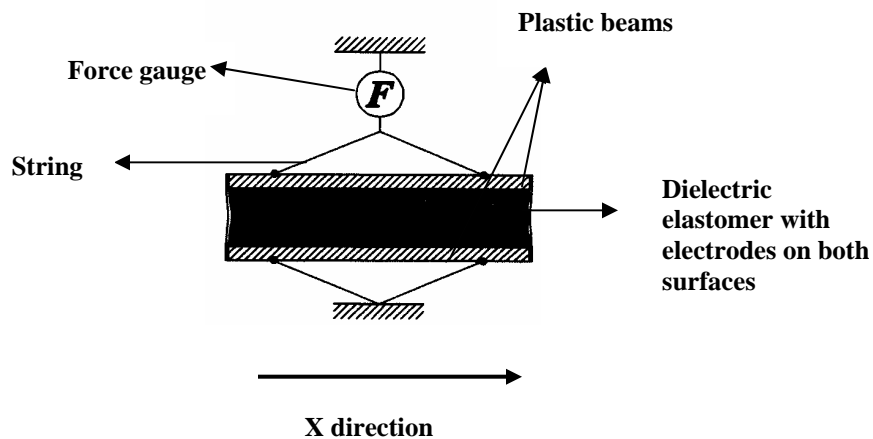


Figure 5: Experiment set-up the x and y directions are horizontal and vertical, respectively [44]

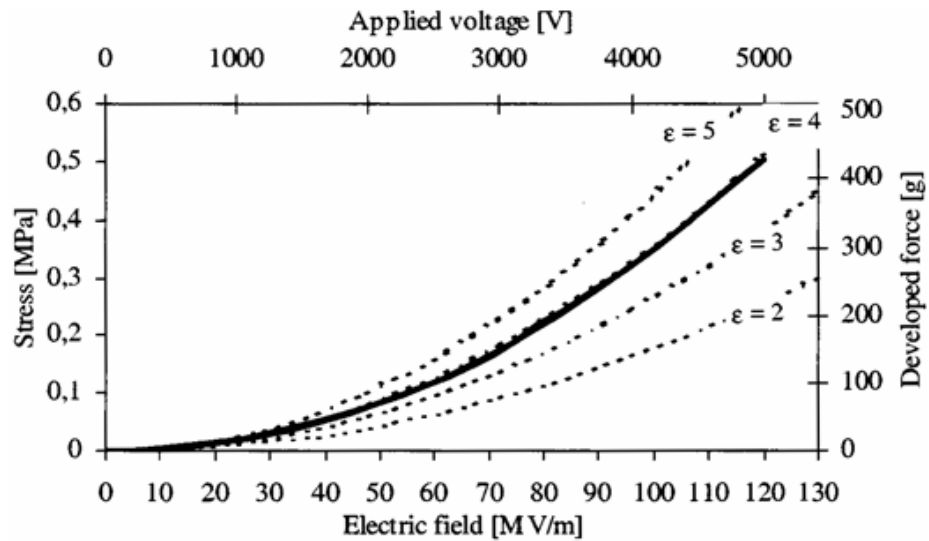


Figure 6: Stress/force vs electric field/voltage curve for sample with 500% x 300% pre-strain [44]

The dielectric constant of the unstrained material is 4.7 according to the 3M literature. The difference was 18%. The 18% lower performance of the actuator was explained by deviations between the test set up (Figure 5) and ideal conditions. They also found that there is a slight tendency for the higher pre-strain curves to produce slightly less force in response to the applied voltage as shown in Figure 7 [44].

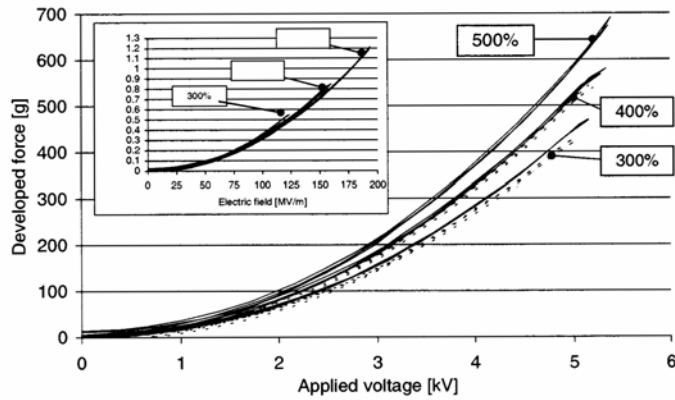


Figure 7: Force/voltage curve for the same sample at different strains in the length direction [44]

Kofod et al. also observed that the electric field that may cause breakdown of the DE depended on the pre-strain ratio. In the unstrained state the breakdown field was 20MV/m, when the film was pre-strained 500% x 500% the breakdown field was reported 218MV/m. Kofod et. al. concluded that the breakdown strength across a polymer chain is higher than along it. The orientation of the polymer chains in the plane of the film due to the pre-strain increases the breakdown strength. Figure 8 shows the relation between the thickness, breakdown electric field and the breakdown voltage [44].

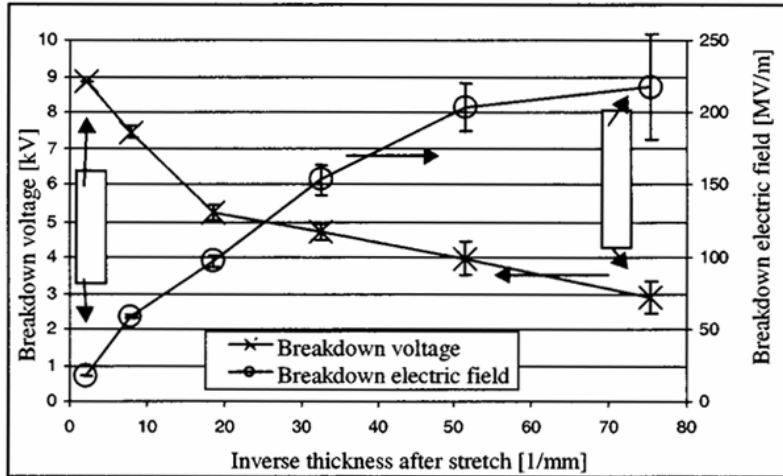


Figure 8: Electrical breakdown strength of isotropically pre-stained acrylic tape [44]

Pelrine and coworkers [50] carried out experiments in order to determine the response of dielectric materials to the applied voltage. They evaluated various silicone films (Nusil Technology's CF19-2186, Dow Corning HS3) as well as one acrylic foam tape (3M's VHB 4910) mentioned earlier. Perline et al [50] reported extraordinarily high levels of actuation strains of 215% for acrylic tape; five to six times those previously reported earlier. They also reported higher pressures (up to 7 MPa) and energy densities about 23 times of those reported earlier for acrylic tape. They attributed the observations to the unique characteristics of VHB 4910 acrylic foam tape, as well as the application of high pre-strain in one planar direction, which enhances electrical breakdown strength and causes the material to actuate primarily in the low pre-strain planar direction.

Linear strain and areal strains measured by Perline et al for the three elastomers under different conditions of pre-strain are given in Table 3. Actuated strains of silicones were greater than for any known high-speed electrically actuated material except VHB 4910

acrylic foam tape. Silicone elastomers also have other desirable material properties such as good actuation pressures and high theoretical efficiencies (80 to 90%) because of the elastomers' low viscoelastic losses and low electrical leakage. The VHB 4910 acrylic elastomer produced highest performance in terms of strain and actuation pressure. Perline et. al. also reported that acrylic films were operated continuously for several hours at the 100% relative area strain level with no apparent degradation in performance. However, it was observed that acrylic elastomer had relatively high viscoelastic losses that limited its half-strain bandwidth to about 30 to 40 Hz in the areal strain test [50].

Table 3: Circular and linear test results for different types of elastomers [50]

Material	Prestrain (x,y) (%)	Actuated relative thickness strain (%)	Actuated relative area strain (%)	Field strength (MV/m)	Effective compressive stress (MPa)	Estimated $^{1/2}ze$ (MJ/m <sup>3</sup> )
<i>Circular strain</i>						
HS3 silicone	(68,68)	48	93	110	0.3	0.098
	(14,14)	41	69	72	0.13	0.034
CF19-2186 silicone	(45,45)	39	64	350	3.0	0.75
	(15,15)	25	33	160	0.6	0.091
VHB 4910 acrylic	(300,300)	61	158	412	7.2	3.4
	(15,15)	29	40	55	0.13	0.022
<i>Linear strain</i>						
HS3	(280,0)	54	117	128	0.4	0.16
CF19-2186	(100,0)	39	63	181	0.8	0.2
VHB 4910	(540,75)	68	215	239	2.4	1.36

In another publication, Pelrine and his coworkers [9] compared natural muscles with various man-made actuators, see Table 4. In order to achieve the important characteristics of natural muscles, actuators must be able to reproduce the features such as power, stress,

strain, speed of response, efficiency, and controllability. They mentioned that electroactive polymer technologies based on electric field induced deformation of dielectric polymers with compliant electrodes is a promising area because of their high strains and energy densities.

Table 4: Comparison of natural muscle and man made actuator technologies [9]

Actuator	Strain	Actuation Pressure	Density	Efficiency	Speed (fast AND slow)
Natural Muscle	●	●	●	●	●
Electromagnetic	●	●	○	●	○
Piezoelectric	○	●	◐	●	●
Shape Memory Alloy	◐	●	◐	○	○
Magnetostrictive	○	●	○	●	○
Electrostatic	●	○	●	●	●
Dielectric Elastomers	●	●	●	●	●
○ = Poor                  ◐ = Fair                  ● = Good					

According to Pelrine et al [9], it is important that an actuator be able to deliver muscle-like performance at common muscle frequencies. They tested various characteristics of natural muscle such as stress, strain and power density at various frequencies and compared it with acrylic elastomer. They found that the acrylic DE actuator fell within the general trend of muscle like performance. Figure 9 shows the strain and stress of DE actuator compared to various natural muscle data points [9].

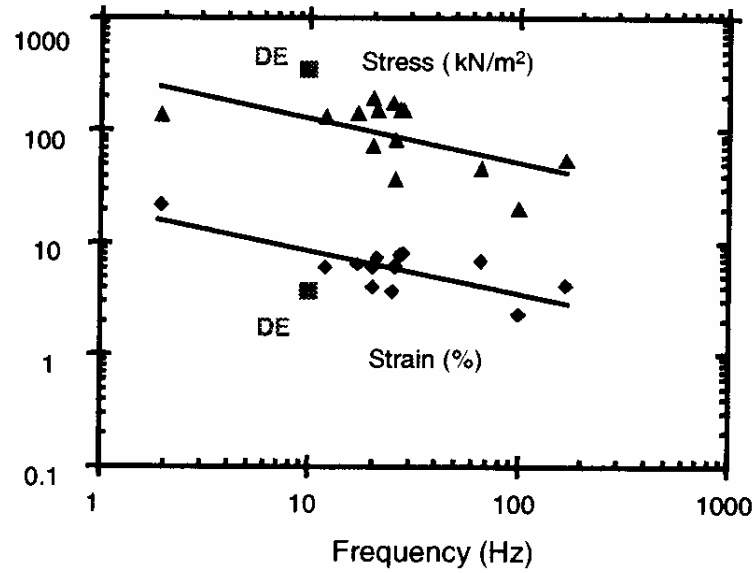


Figure 9: Strain and stress of DE actuator compared to various natural data points [9]

Perline et al [9] also compared power density and work-per cycle performance of natural muscle and acrylic DE actuators. They found that the measured performance of the relevant parameter falls within the general trend of natural muscle. Figure 10 shows the power density and work-per cycle for DE actuator compared to natural muscle data points.

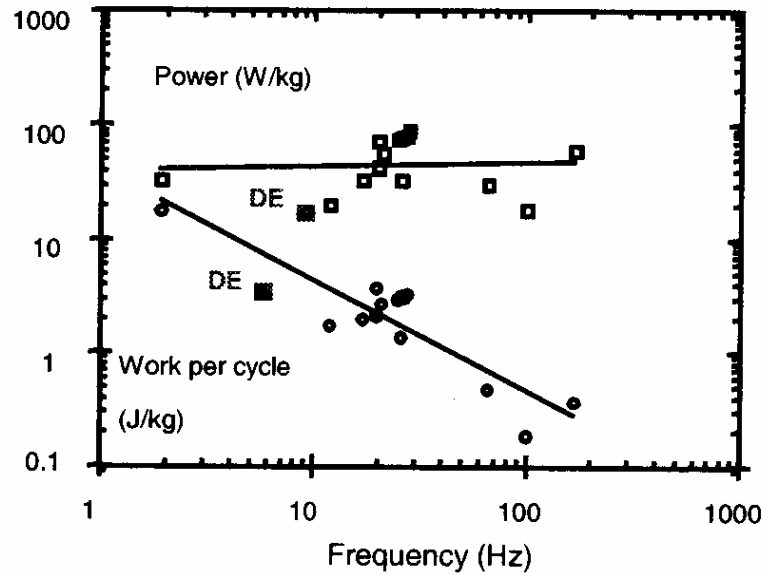
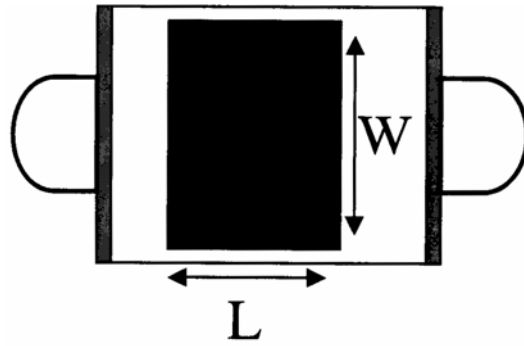
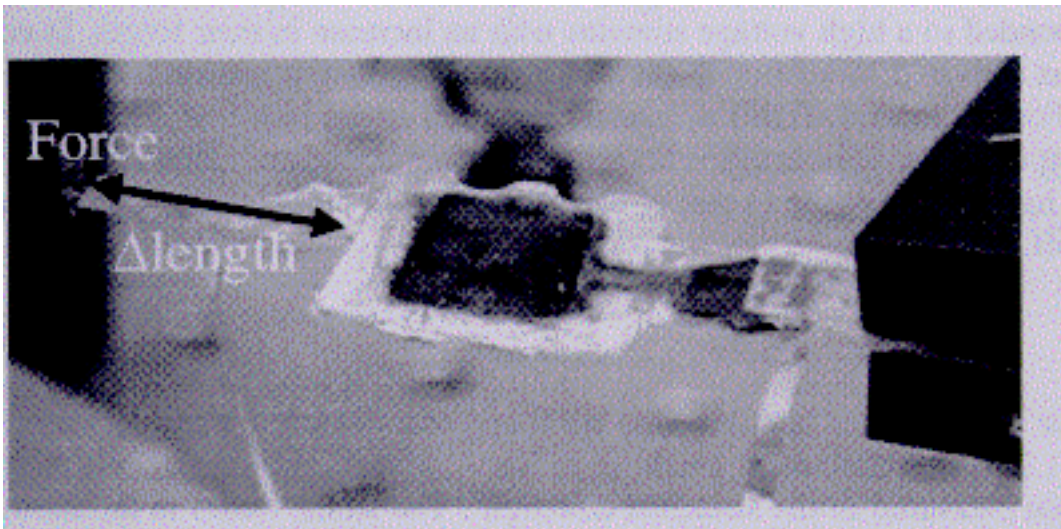


Figure 10: Power density and work-per cycle for DE actuator compared to natural muscle data points [9]

Meijer et al [51] studied the performance of different actuators based on EAP technology and compared them with the human muscle. Two of the DE they tested were 3M's VHB 4910 acrylic tape and NuSil Technology's CF 19-2186 silicone material. Both of the films were coated with carbon grease (CW 7200 of Chemtronics Circuit works) compliant electrodes. Figure 11 and 12 shows the actuator design and the experimental set up respectively. Acrylic film and silicone film were glued to a wooden support system (see Figure12) at a 1.5 N pre-tension and 1 N pre-tension respectively. The experimental set up they used consisted of a muscle lever system that can simultaneously record position and force. One side of the EAP actuator was connected to the muscle lever and the other side was rigidly fixed with a clamp, see Figure 12.



*Figure 11: Schematic design of the actuators [51]*



*Figure 12: Picture of the acrylic dielectric elastomer actuator. The black arrow indicates the length changes that were imposed on the actuator by the muscle lever. [51]*

The EAP material was activated using an electrical circuit that generated square wave high voltage (0-5kV) pulses of varying duration (10-500 ms). A personal computer controlled the timing of the stimulation to the EAP actuator.

In order to characterize the mechanical performance of the actuators, Meijer et al [51] evaluated the isometric stress and examined how the actuators used their capacity

when they performed work on the environment. Isometric force was defined as the maximal change (increase or decrease) in force that could be attained with an applied stimulus. Isometric stress was calculated by normalizing the force to the area perpendicular to the force direction. They concluded that maximal isometric stress of the dielectric elastomers in the stretch direction were all within the range found for biological muscle. Figure 13 shows the graphs for acrylic elastomer and silicone elastomer [51]

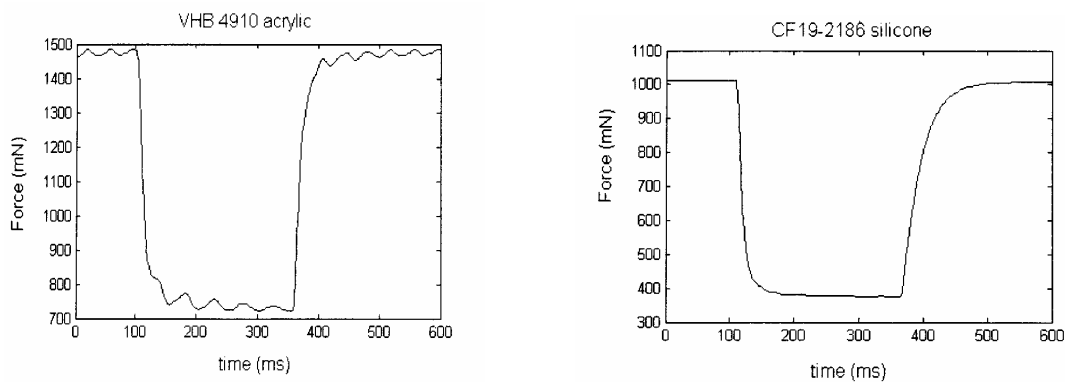


*Figure 13: Maximal isometric contractions of the tested actuators [51]*

In addition Meijer et al [51] evaluated the generation of work and power in the actuators. First they evaluated the passive work-loops of the actuators when they were not stimulated as shown in Figure 14.

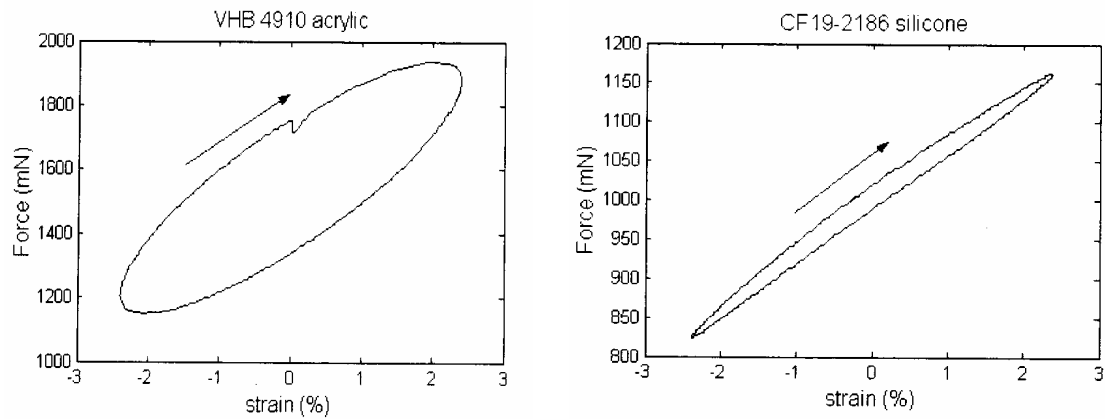


*Figure 14: Passive workloops of the tested actuators at an oscillatory frequency of 2Hz [51]*

In order to have the DEs generate positive work, the actuators needed to be stimulated during the lengthening phase of the workloop. This resulted in a small force during lengthening and a larger force during shortening and hence the generation of work. Figure 15 shows the active workloops that maximized work output. Meijer et al found that maximum work output was attained at a strain of 5%. Despite the large visco-elastic losses the acrylic actuator still generated large work outputs. Table 5 shows the comparison of two dielectric elastomer with natural muscle [51].

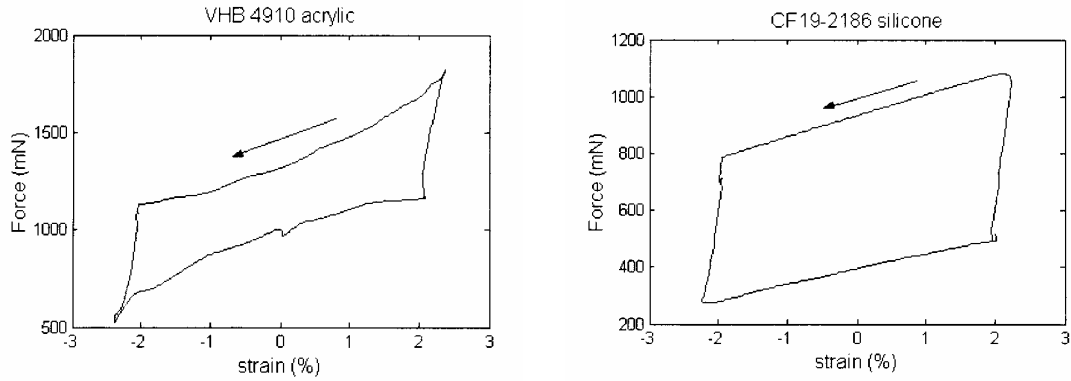


Figure 15: Active workloops of the tested actuators at an oscillatory frequency of 2Hz. [51]

Table 5: Comparison of natural muscle and man made actuator technologies [51]

Actuator	Biological muscle <sup>(9)</sup>	VHB 4910 acrylic	CF19-2186 silicone
Cross sectional area (mm <sup>2</sup> )	-	1.26	3.76
Preload (g)	-	150	100
Action upon stimulation	contraction	extension	extension
Strain (%)	1-100	215 <sup>(5)</sup>	63 <sup>(5)</sup>
Isometric stress (MPa)	0.007 - 0.8	0.60	0.15
Max Work output (J/kg)	0.18 - 40.57	13.17	3.19
Max Power output (W/kg)	9 - 284	35.28	20.37
Frequency (Hz) at max Power	1.9 - 173	4	10

## 2.3 Compliant Electrodes

As mentioned before dielectric elastomer actuators consist of a thin film between two electrodes. One of the main characteristics of dielectric elastomer actuators, maybe the most important one, is their high actuation strain. To accommodate the high strain during

actuation the electrodes around the DE should also deform without imposing any restraints while maintaining their conductivity. In other words the electrodes have to be compatible with the DE in their mechanical properties. Therefore the compliant electrode is a key feature of the DE actuator technology.

In addition to mechanical properties such as elastic moduli, hysteresis, etc., other properties such as conductivity, percolation, are also of importance. Compliant electrodes should conform to the shape of the DE they are attached to. The electrodes must stretch in at least one planar direction of the film while its thickness contracts; otherwise actuation will be dramatically reduced. The electrode system should follow the strain of the actuator system without generating opposing force, while maintaining its conductivity during the actuation. In summary the mechanical behavior of the desirable compliant electrodes are critical for the performance of the actuator must be compatible with the dielectric polymer behavior, in that these must accommodate large deformation without substantial loss of conductivity under repeated deformation cycles. Compliant electrodes should be thin and should be easily patternable as well [52, 53].

Many types of compliant electrodes used in conjunction with DE actuators have been reported in the literature. Among them are particle included polymers, metals, and conductive polymers. Particle included polymer based electrodes generally consist of carbon or silver as particles and a polymer medium such as silicone. Traditionally, these have been classified as grease and rubber electrodes [4, 39, 49, 52, 53].

### *2.3.1 Grease and Rubber Electrodes*

The distinction between grease and rubber electrode type is their preparation techniques and application methods.

Grease electrodes consist of a carrier polymer and powdered graphite particles. To prepare grease electrodes, a suspension of graphite in a solvent (for the polymer media), prepared using ultrasound is added to polymer carrier (in compatible solvent). Ketjenblack® EC-300J (produced by Akzo Nobel) can be used as graphite and silicone materials can be used as polymer carrier. Both for polymer carrier and graphite, heptane can be used as solvent. Than mixture is placed in a fume hood to allow the solvent to evaporate. The evaporation process is interrupted at the optimum application viscosity level. Grease electrodes can be applied on the film with a brush [52, 53].

Rubber electrodes also consist of a carrier polymer and powdered graphite as conductive particles like grease electrodes. Once again, a suspension of graphite in solvent (for the carrier polymer), prepared using ultrasound is added to polymer carrier. The component materials described earlier for grease electrodes can also be used for rubber electrodes. The low viscosity mixture can then be sprayed with an airbrush on dielectric films to form rubber electrodes [52, 53].

Toth and Goldenberg [54] characterized the variation in impedance of various electrodes as a function of stretch. A schematic diagram of their experimental set up is shown in Figure16. The electroded film was stretched in increments of 25% and the impedance was measured between the reference node and each of the measurement points at each state of stretch. Figure 17 shows the measured resistance for a carbon grease electrode reported by Toth and Goldenberg [54].

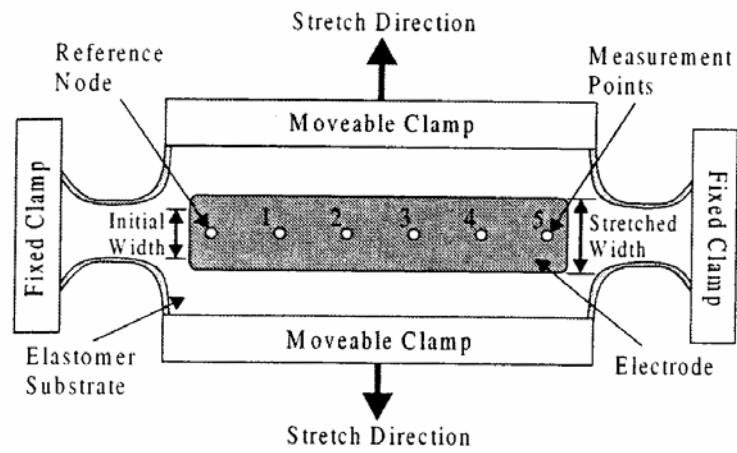


Figure 16: Schematic diagram for the testing of the electrode resistance [54]

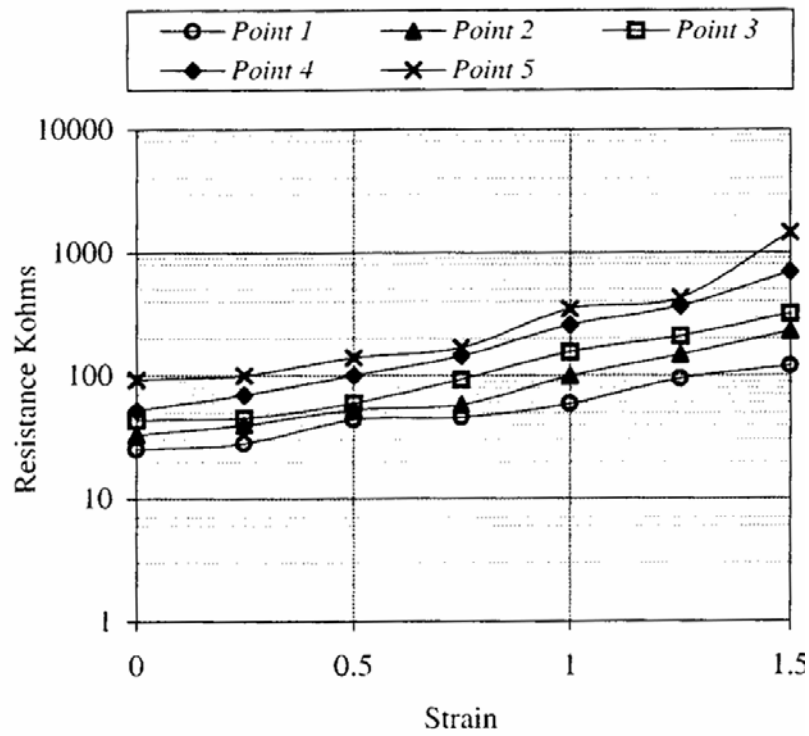


Figure 17: Electrode resistance versus strain [54]

Toth and Goldenberg [54] also found similar relationships for other electrode materials which were carbon conductive grease (CW 7100 from Chemtronics), conducting RTV silicone (RTV 60-CON from General Electric), for silver conducting grease (CW 7300 from Chemtronics), and graphite powder (S4). They expressed their empirical observation of strain-resistance relationship as;

$$\log R = b(\alpha - 1) + c$$

where b and c are experimentally determined constants and  $\alpha$  is the stretch ratio. They rewrote this equation as

$$R = R_0(\beta)^{(\alpha-1)} \quad \text{and} \quad \beta = \frac{R_i}{R_0}$$

where  $R_0$  and  $R_i$  are the resistance measured at  $\alpha$  equal to 1 and  $\alpha$  equal to 2 respectively. Since  $\alpha$  represents the stretch ratio, when  $\alpha$  is equal to 1, there is no stretch on the DE film. When  $\alpha$  is equal to 2, there is 100% stretch on the DE film. If  $\beta$  is high, it means the electrodes lose their conductivity when the film is stretched.

Toth and Goldenberg [54] calculated values of  $\beta$  for some common electrode materials: 4 for carbon conductive grease (CW 7100), 6.5 for conducting RTV silicone (RTV 60-CON), 6.8 for silver conducting grease (CW 7300), and 22 for graphite powder (S4) [54].

Faltdt and Kofod [53] investigated dielectric spectroscopy of graphite filled silicone rubbers. They carried out measurement of conductivity of silicone having various graphite

content. The samples were prepared as a mixture between graphite powder (4206 Merck, Germany) and Dow Corning Sylgard 184. Samples were cast from a heptane solution directly on to glass plates. Samples of thickness ranging from 500  $\mu\text{m}$  to 1000  $\mu\text{m}$  were prepared with graphite content in percentages from zero to 30% in steps of 1%. Faldt and Kofod [53] found that the conductivity changes significantly between the samples with 23% and 24% graphite. Figure 18 shows the results of percolation experiments according to the graphite percentage by volume. For low graphite content, the graphs have a constant slope of  $\sim 1$ . For percentages higher than 23%, the graphs have a constant plateau at low frequencies, but at higher frequencies they return to a slope of  $\sim 1$  [53].

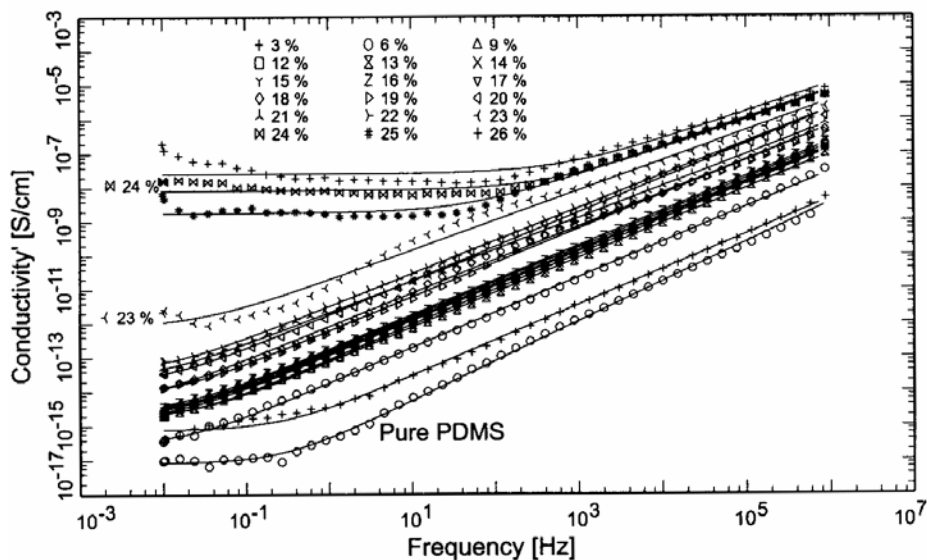


Figure 18: Percolation experiment graphs for Sylgard 184 with different percentages [53]

Kofod [53] evaluated two types of compliant electrodes, identified as rubber and grease. In his experiments, he used Ketjenblack EC-300J as graphite (produced by Akzo Nobel) and different silicone materials as polymer carrier in order to prepare grease and

rubber electrodes. The difference between these two electrode types were their preparation and application techniques.

For grease electrodes Kofod [53] used silicone (Sylgard 184) and viscosity lowering agent Dow Corning 200FL 50 cst mixtures. Kofod prepared the electrode mixtures with the graphite volume percentages of 3%, 5%, 10% and 20%. Kofod reported relatively high resistance values for 3% graphite content, mixture containing 5%, 10% and 20% graphite were all conductive. In terms of ease of application (by smearing on the film), mixture containing 5% graphite showed the best results followed by the 10% mixture. The mixture containing 20% graphite was difficult to apply on the DEfilm. In case of rubber electrodes Kofod tested several types of silicone with Wacker E43 RTV-1 silicone glue. In case of rubber Kofod used only 20% graphite content [53].

As for dielectric material, Kofod [53] worked on 3M's VHB 4910 acrylic tape and different types of silicone films. Dow Corning Sylgard 184 and 186, Wacker Elastasil were some of them. Kofod used rubber and grease electrodes only for silicone films, not for VHB 4910 acrylic tape. He claimed that, since silicone sticks to silicone, rubber and grease electrodes were suitable only for silicone films [53].

### *2.3.2 Conductive Polymer Electrodes*

Electrically conducting polymers are a relatively new class of electronic materials that may be considered as potential candidates for the required electrodes. These polymers have the potential of combining the electrical properties of metals with the processing advantages of conventional polymers. Some of the examples of conductive polymers are polypyrroles, polyanilines, and polyacetylenes [55, 56, 57, 58].

Cheng Z. Y et al [55], Su J. et al [56], Kuhn et al [57], Watanabe M. et al [58] reported that polypyrrole is a conductive polymer and can be used as compliant electrodes for the dielectric elastomer actuator systems. Details of their findings will be discussed later. Polypyrrole can be easily polymerized by using ferric chloride ( $\text{FeCl}_3$ ) in aqueous medium in the presence of dopants such as sodium salt of anthraquinone-2-sulfonic acid or 5-sulfosalicylic dihydrate. By using in-situ deposition technique it is possible to form a conductive polymer coating on the dielectric elastomeric films [55, 56, 57, 58] . When a dielectric polymer film come in contact with an aqueous solution of an oxidatively polymerizable pyrrole compound, oxidizing agent react with the pyrrole compound and form a conductive polymer coating on the dielectric material. Polypyrrole electrodes will be discussed later

Kuhn [56] published a patent about the depositon of polypyrrole to the textile materials. Polypyrrole electrodes can be deposited on to the dielectric material by chemical oxidation of pyrrole in an aqueous solution, which is called in-situ deposition technique. The object of the invention was to provide a conductive textile material by depositing pyrrole to the surface of the material. Patent recommends anthraquinone-2-sulfonic acid as doping agent and also they claimed that a large excess of dopant is not required to achieve high conductivity. Another advantage of the invention is the coating has superior stability [56].

Ji Su et al [57] used in-situ deposition technique, which was described at section 2.3.2, to form polypyrrole electrodes on polyurethane films. They evaluated polypyrrole electrodes and compared them with gold electrodes. Ji Su et al found that the interface between polyurethane and polypyrrole electrodes is coherent and that the PPy electrodes had improved acoustic and optical transparency compared to the gold-electroded

polyurethane films. On the dielectric properties, they reported similar behavior for gold and PPy electrodes. In addition, they found that under identical measurement conditions, the large electric field induced strain responses and the characteristics of the thickness and frequency dependence properties of both were similar as well [57].

Watanabe et al [58] reported on formation of wrinkled polypyrrole electrodes on polyurethane films. The premise for the geometry was two-fold; first conductivity of the electrode would not decrease with the field-induced surface extension of the actuator and the second was that the electrode would not constrain the actuation. They prepared the wrinkled polypyrrole electrodes through in situ deposition technique (as used by Ji Su et al [57]). Watanabe et al prepared the wrinkled electrode on uniaxially strained (0-35.3%) polyurethane films as shown in Figure 19. The strained film was then placed in a reaction mixture of pyrrole to coat the film with the PPy electrode. After the reaction, the strain was released, which made the electrode wrinkle because PPy is much less elastic than the polyurethane. Electrical resistance of the electrode on the polyurethane film was measured while the electrode was elongated using the frame. Watanabe et al reported that the wrinkles enabled the electrode to elongate without decrease in conductivity. Figure 20 shows the resistance of the PPy electrodes under different conditions. According to the test results, Watanabe et al reported that in the electrode prepared on the undrawn polyurethane film, the resistance exponentially increased with the elongation, see Figure 20 a. In the electrode prepared on the 35.3%-drawn polyurethane film, the resistance was almost constant at elongation rates less than 40%, see Figure 20 e [58].

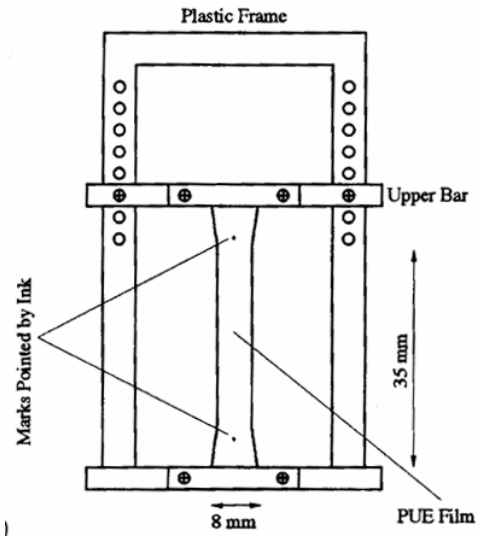


Figure 19: Frame for drawing the PUE film [58]

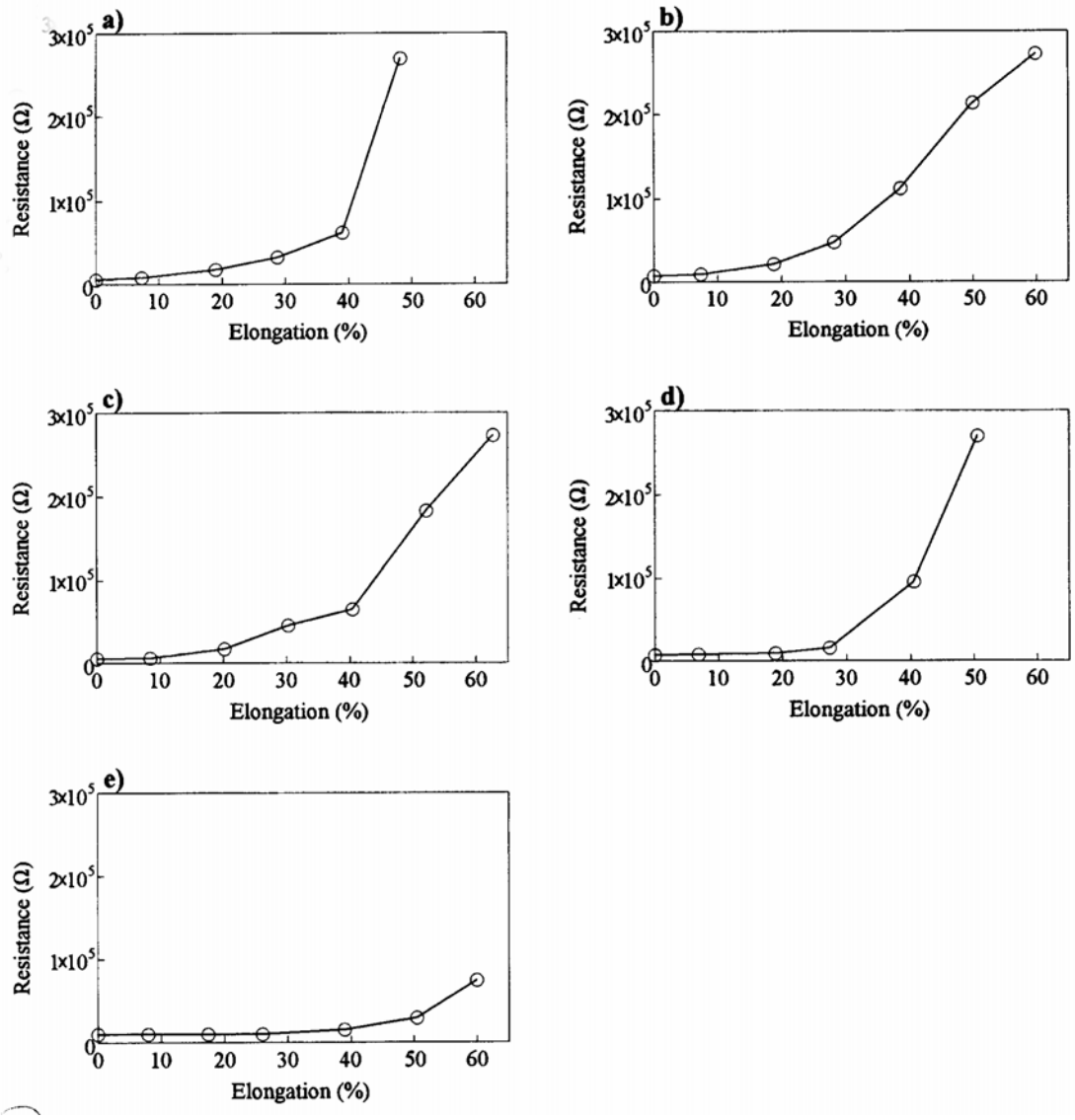


Figure 20: Resistance of the PPy electrode under elongation. The electrodes were prepared a) undrawn, b) 9.8% drawn, c) 17.9% drawn, d) 28.2% drawn, e) 35.3% drawn PUE films [58]

Watanabe et al [58] also reported that the wrinkled PPy electrodes improved the bending-electrostrictive actuation of the polyurethane film. In order to evaluate the difference between the wrinkled PPy electrodes and unwrinkled PPy electrodes Watanabe et

al first prepared three samples (sample A, B and C) that had (unwrinkled) electrodes of different thickness. To vary the thickness, Watanabe et al repeated the deposition of PPy twice in Sample B and three times in Sample C. In Sample A, it was carried out only once. The thickness ratio of the electrode was supposed to be Samples A:B:C=1:2:3. Watanabe et al reported that the field induced displacement of Sample A was much larger than that of Sample C, which means that the PPy electrode could constrain the bending actuation of the polyurethane film, see Figure 21. Watanabe et al thought that the wrinkled PPy electrode did not constrain the actuation because it could apparently elongate by smoothing the wrinkles. Watanabe et al reported that the displacement of the film with the wrinkled electrode was more than twice that of the film with the unwrinkled one, see Figure 22.

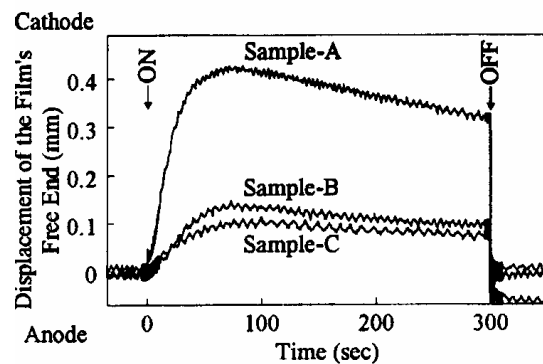


Figure 21: Field induced displacement of the PUE films with PPy electrodes of various thickness [58]

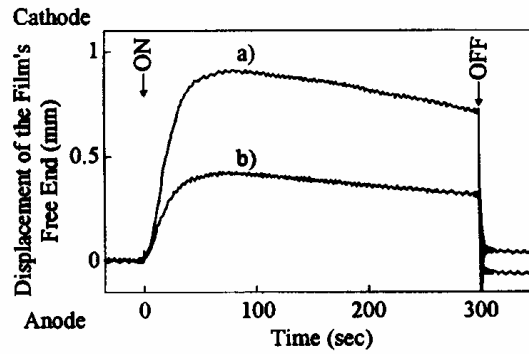


Figure 22: Field induced displacement of the PUE films with a) the wrinkled PPy electrode and b) the unwrinkled one. The wrinkled electrode was prepared on the 10.5% drawn PUE film [58]

It is important to note that they also found improved actuation with doping of the polyurethane with sodium acetate. Figure 23 shows the field-induced bending of the film. Watanabe et al reported that the wrinkled PPy electrode significantly improved the displacement as compared with the unwrinkled one, see Figure 23 a and b. By comparing Figs 22 and 23, the doping also improved the displacement [58].

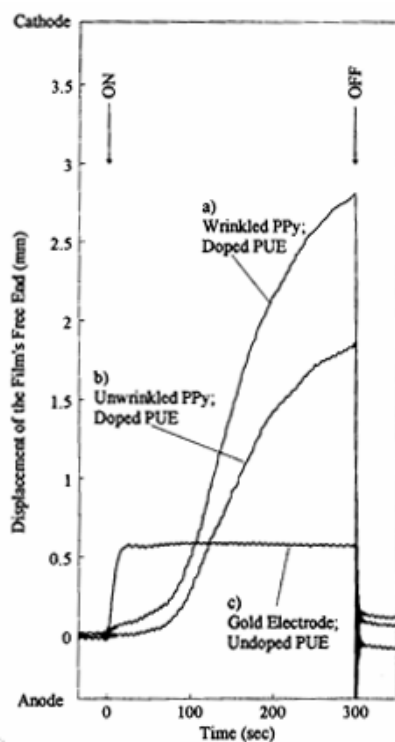
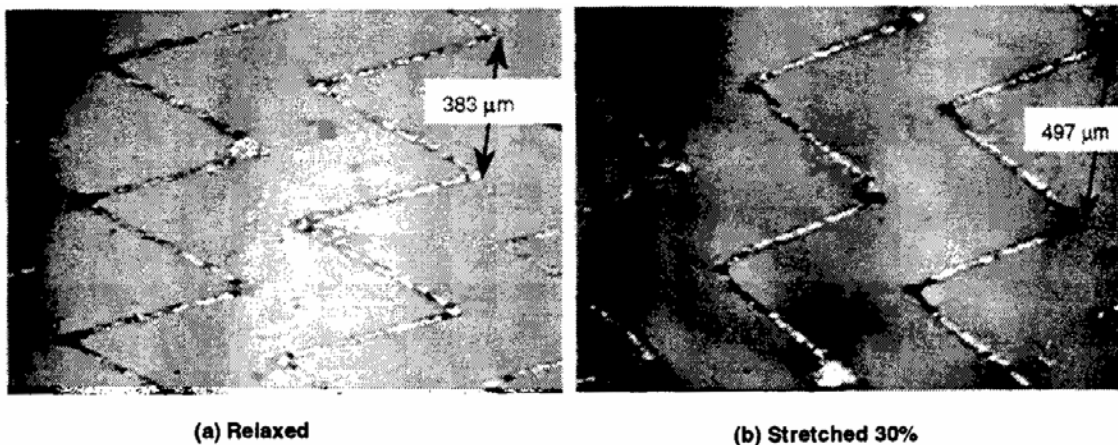


Figure 23: Field induced displacement of a) the doped PUE film with the wrinkled PPy electrode prepared on the 9.9% drawn PUE film, b) the doped PUE film with the unwrinkled PPy electrode and c) an undoped PUE film with a conventional gold electrode [58]

### 2.3.3 Metal Electrodes

Metals such as gold, silver and aluminums have been used to fabricate compliant electrodes [4, 39, 49, 54]. These classes of compliant electrodes have high acoustic impedance and impose mechanical constraints on the soft polymer DE that can significantly reduce the electromechanical efficiency of the actuator. Metal electrodes have been deposited by evaporative or sputtering processes. Generally, because of their high stiffness, it is not possible to reach high strain levels with these class of electrodes [4, 39, 49, 54].

Kornbluh and co-workers [4] reported, sputter-deposited ultrathin gold electrodes with thickness below 0.1mm. They reported that uniform gold electrodes easily crack and strains greater than about 4% are difficult to achieve. As a remedy, they used patterned electrodes rather than uniform gold electrodes and claimed that this structure could remain conductive at much greater film strains. In their experiment, Kornbluh et al [4] used zigzag patterns of sputtered gold traces uniformly on silicone films and then patterned via photolithography, and gold traces were fabricated with line widths as small as  $5\mu\text{m}$ , see Figures 24 and 25. They found that these electrodes remain highly conductive at film strains up to 80%. Kornbluh et al [4] also mentioned that a second electrode material is needed to carry the charges in between the zig-zag traces, for uniform distribution over the surface of the polymer. The second electrode material can be any weakly conductive but soft material. It can be a polymer filled with conductive particles such as fine carbon or it can be an ionically or electronically conductive polymer [4].



*Figure 24: Zig-zag cold electrodes [4]*

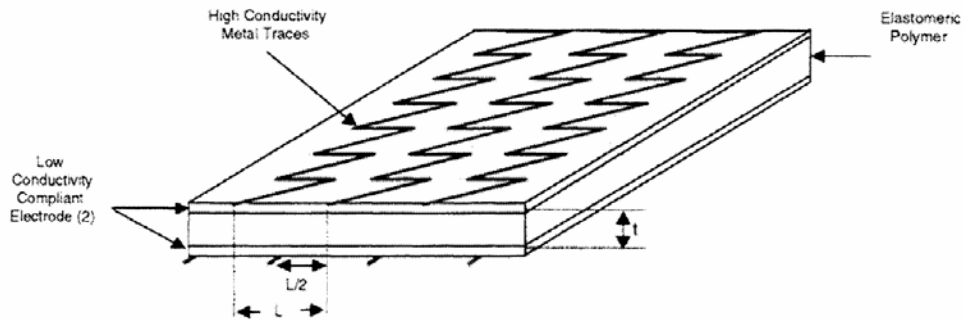


*Figure 25: Structured electrodes [4]*

Benslimane and Gravesen [49] worked on smart metallic compliant electrodes on silicone elastomer Elastosil RT 625 (a Wacker product). They used thin layers of silver films as compliant electrodes on the elastomer films, spin cast on a mould with a micrometer sized 3D pattern, see Figure 26. Upon curing and subsequently releasing of the film from the mould, the pattern was replicated to one side of the film, while the other side remained flat. By spin casting silicone films on a mould, which had a cross section as shown in Figure 26 they formed a corrugated surface profile. Figure 27 shows the schematic of the actuator with smart metallic compliant electrode. The electrode was compliant in the direction of the wave-pattern but it was as stiff as a metallic layer in the perpendicular direction to the corrugation. The corrugation depth to period ratio was optimized in order to obtain elongations of about 33% before the metallic electrode breaks, and this corresponded to a ratio of about 0.4. They used 4-micron deep corrugation (top to bottom) with a period of 10 microns. They found that compliant metallic electrodes maintained conductivity up to 33% expansion before breaking and losing electrical connectivity [49].

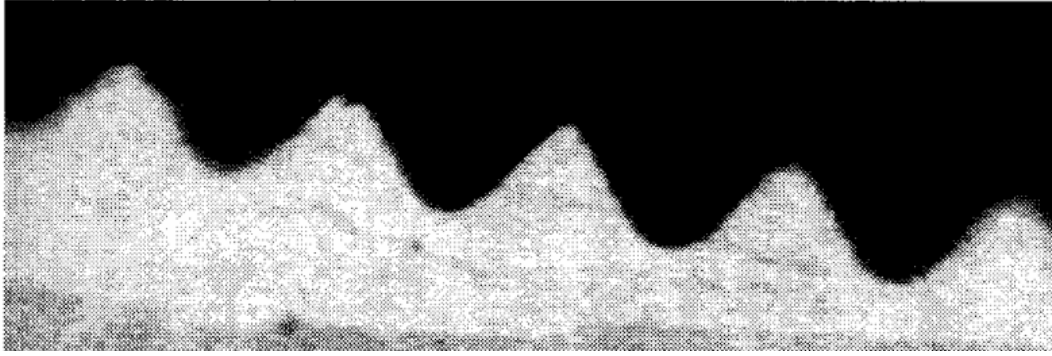


Figure 26: Optical microscope picture of the cross-section of a mould [49]

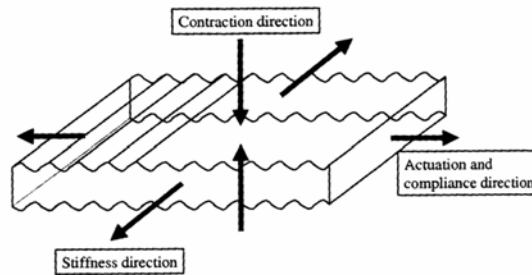
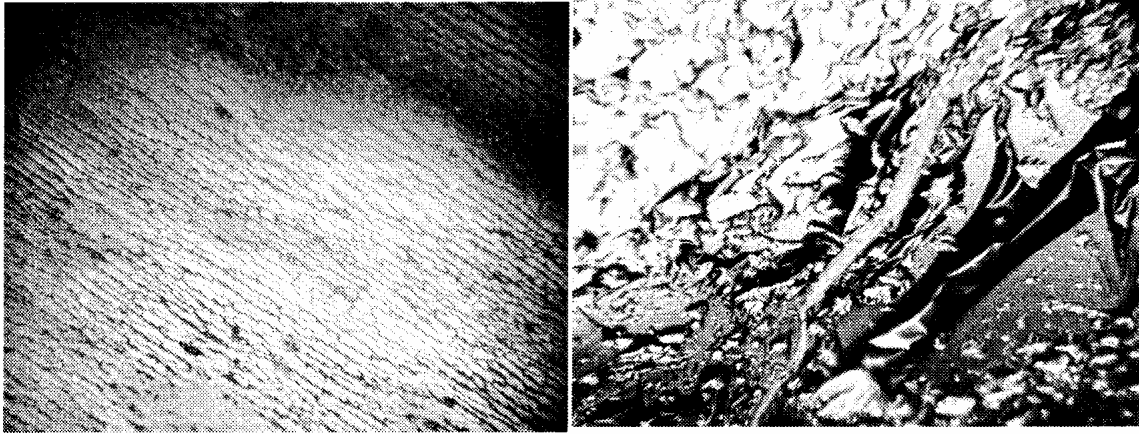


Figure 27: Schematic of an elastomer actuator/sensor [49]

Kim et al [39] reported on formation of gold electrodes on electroactive paper using sputtering and evaporation techniques. Electroactive paper actuators were made with a chemically treated paper by constructing electrodes on both sides of the paper. When electrical voltage was applied on the electrodes the electroactive paper actuators produced bending displacement.

Extremely thin gold film electrode was prepared with sputtering process, see Figure 28. However, they reported that after a few tests the electrodes either cracked or wrinkled. They found that cellophane papers with gold electrodes exhibited a remarkable

displacement output. They applied a 2 kV/mm of excitation voltage to a 30mm long paper beam and observed more than 3 mm of tip displacement [39].



*Figure 28: Photographs of gold sputtered electrodes [39]*

Kim et al [39] also used evaporation technique in order to prepare gold electrodes, see Figure 29. These electrodes showed less cracks than sputtered films, and thus required reduced activation voltage. Since by using evaporation technique, electrodes were produced at relatively low temperatures, suitable for papers, Kim et al claimed that evaporation technique was better than sputtering [39].

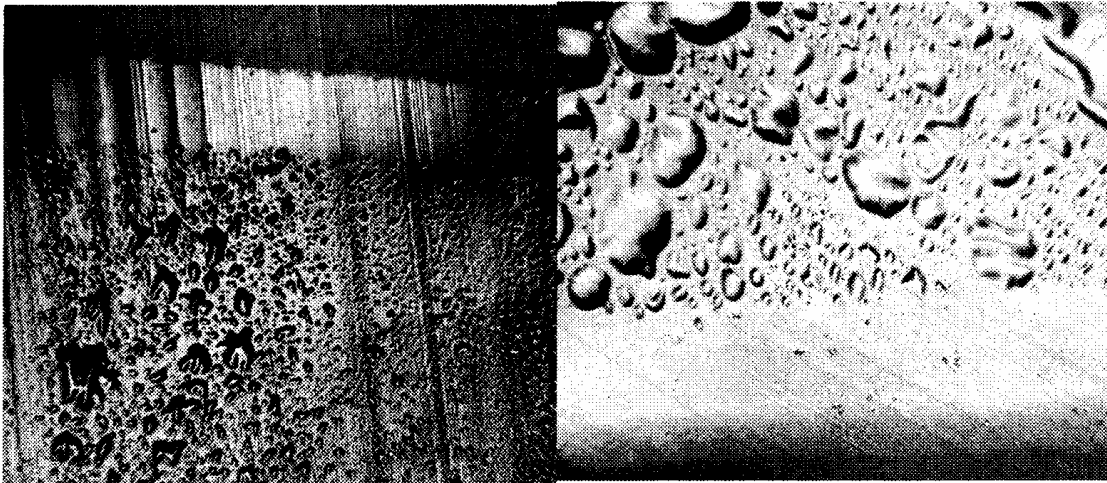


*Figure 29: Photographs of evaporation-deposited electrodes [39]*

Cheng et al [55] studied conductive polymers, polypyrrole and polyaniline as compliant electrodes and compared some performance characteristic of these electrodes with gold electrodes. Two different electroactive polymers, Poly(vinylidene-trifluoroethylene) P(VDF-Tr-FE) of high elastic modulus and polyurethane of low elastic modulus were used for all the actuators. Comparison of actuators which had conductive polymer electrodes and gold electrodes showed that longitudinal strain response of the actuators which had conductive polymer electrodes was nearly the same as the actuators which had gold electrodes. However, the transverse strain response of the all polymer electrostrictive system was much better than that with gold electrodes. They concluded that, since the acoustic impedance of the conducting polymer is nearly the same as that of the electrostrictive polymer, the same or higher electric field induced strain responses of the all polymer system indicated that a high performance actuator and transducer can be obtained with the all polymer electrostrictive system [55].

### **3 Research Objective**

The objective of this research is, to characterize various compliant electrodes on dielectric elastomer EAPs under different process conditions. Characterization of the electrodes includes their response to applied voltage, their conductivity values under different test conditions and their topography. Three different types of compliant electrode have been characterized. These were rubber electrodes, grease electrodes and polypyrrole electrodes.

## 4 Experimental

The need for conformable electrodes for further development of EAP actuators is very clear and the desired characteristics of these are well defined. The experiments for fabrication and evaluation of the conformable electrodes are described in this chapter. The observations will make it easier to optimize the material and process related issues.

### 4.1 Materials

As mentioned at section 3, three different types of compliant electrode have been characterized. These were rubber electrodes, grease electrodes and polypyrrole electrodes.

#### *4.1.1 Grease and Rubber Electrodes*

For grease and rubber electrodes consisting of a carrier polymer and powdered graphite, three different types of silicone material were evaluated. These were; Sylgard®184, Sylgard®186, and Nusil CF19-2186. Nusil CF19-2186 is a two-component silicone elastomer, which is a product of Nusil Technology. Also both Sylgard®184 and Sylgard®186 are two component silicone elastomers as well and they are manufactured by Dow Corning. Fluid 200® FL 50 CST is another Dow Corning product and used as viscosity lowering agent for Sylgard®184 and Sylgard®186 silicones. As for graphite Ketjenblack® EC-300J have been used, which is produced by Akzo Nobel. Heptane, which is produced by Fischer Scientific was used as a solvent for all the silicone elastomers and graphite.

#### *4.1.2 Polypyrrole Electrodes*

In order to form polypyrrole electrodes, conductive polymer pyrrole 98% was used for the experiments. Pyrrole can be polymerized in the presence of dopants and oxidizing

agents. In the present research ferric chloride ( $\text{FeCl}_3$ ) has been used as oxidizing agent and sodium salt of anthraquinone-2-sulfonic acid and 5-sulfosalicylic acid dihydrate have been used for doping polypyrrole.

### *4.1.3 Dielectric Elastomer*

3M VHB™ 4910 double coated acrylic foam tape has been used as dielectric elastomer. VHB 4910 is a very high bond structural adhesive from 3M. This material has been used by many researchers since it has produced the greatest strains and elastic energy density of any known dielectric elastomer material. The VHB 4910 tape is available as a 1 mm thick sheet, mounted on a red plastic liner, which makes it very easy to cut to the preferred dimensions. Due to its stickiness it is very easy to stretch and mount on frames, making it a very good material for experimentation. The film is translucent and extremely compliant and can be stretched very far in both directions in the plane of the film.

## **4.2 Actuator Fabrication**

Actuators have been fabricated for evaluation of their response in circular form much like many previous investigators [50]. It is important to note that other characterizations for various electrodes have been carried out on electrodes deposited on to the dielectric film while the dielectric film was on the glass slides.

The actuator fabrication process involved pre-straining the dielectric film and subsequently depositing the electrodes on the stretched film. In the experiments described here same nominal pre-strains (250% x 250% in the XY directions) have been used in all cases. The pre-straining of the film has been done on an experimental jig. The circular actuators are of the same dimension (150 mm diameter dielectric film with 35mm in diameter electroded area in the center) in all cases except for those containing polypyrrole

electrodes (97mm diameter dielectric film with 14mm in diameter electroded area in the center)

#### 4.2.1 Preparation and Application of Electrodes

As mentioned before three different types of silicone elastomers were evaluated as matrix material for these electrodes. These were; Sylgard®184, Sylgard®186, and Nusil CF19-2186. Sylgard®184 and Sylgard®186 were mixed at a 50/50 ratio with Fluid 200® FL 50 CST to lower viscosity of the solution wherever needed. The amount of solids or graphite added by weight, were calculated as suggested by Kofod [53].

$$m_{KB} = \left( \frac{\rho_{KB}}{\rho_S} \right) \left( \frac{P_{KB}}{(1 - P_{KB})} \right) m_S$$

Where;

$m_{KB}$  Amount of graphite

$\rho_{KB}$  Density of graphite

$\rho_S$  Density of silicone

$P_{KB}$  Desired volume fraction of graphite

$m_S$  Amount of silicone

All of the density values were obtained from manufacturers' literature; for Ketjenblack® EC-300J it is 1.75 g/ml. The silicone materials, which were used in this research, comprised of two components. Dow Corning's technical data on papers give the

density of these components separately. So it is important to know the density of the mixtures.

The density of the mixtures was calculated according to the formula below;

$$d = \frac{m}{v}$$

Where,

d is density

m is mass of material

v is volume

The density of Nusil CF19-2186 was found 1.1 g/ml. As mentioned before Sylgard®184 and Sylgard®186 were mixed at a 50/50 ratio with Fluid 200® FL 50 CST. The density of Sylgard®184 and Fluid 200® FL 50 CST was found 1.02 gr/ml and the density of Sylgard®186 and Fluid 200® FL 50 CST was found 1.01 gr/ml.

#### 4.2.1.1 Rubber Electrodes

In the first step in preparation of rubber electrodes, required amount of graphite powder was suspend in 50 ml heptane in a container and subjected to ultra-sound treatment for 1 hour in order to break the carbon particles. The required amount of the silicone elastomer was dissolved in 40 ml heptane, separately. The graphite suspension in heptane and the silicone solution were poured into another container and an additional 110 ml heptane. The resulting mixture can be stored at least a month without degradation [53]. Before applying the electrode on to the dielectric film, the mixture is stirred for about 5 minutes with a magnetic stirrer in order to have a uniform distribution of particles before application.

Thin layer of the above mixture was applied with an airbrush to the dielectric film in order to form the rubber electrode. Any commercially available air-spray gun capable of delivering the mixture should be appropriate for this. In this instance Campbell Hausfeld air spray gun was used.



*Figure 30: Air gun*

As mentioned earlier the diameter of circular electroded region was 35 mm in all cases. To apply the rubber electrodes both sides of the dielectric film were masked with plastic films (polyurethane films used in this case) before applying electrodes using the air gun see Figure 31 a. The mixture was sprayed on the dielectric film in a fume hood. The plastic films were separated easily from the dielectric film after applying the electrodes. Figure 31 b shows the final actuator picture after applying electrodes



*Figure 31: a) Film with mask b) Final actuator*

#### 4.2.1.2 Grease Electrodes

The preparation of graphite suspension and silicone solution in heptane for grease electrode material involves the same steps as described for rubber electrodes. In preparing grease electrode these two mixtures are mixed with each other without further addition of heptane and this mixture was subjected to ultra sound treatment for about 10 hours. Subsequently, the mixture is placed in a fume hood to allow the solvent to evaporate. The evaporation process is interrupted at the optimum application viscosity level. It takes more than two days in order to get an optimum application viscosity level. Grease electrodes can be stored at least a month without degradation.

The resulting grease electrodes can be applied to the masked dielectric film with a brush. The masking process is similar to that described for rubber electrodes earlier.

#### 4.2.1.3 Polypyrrole Electrodes

Pyrrole can be polymerized in the presence of dopants and oxidizing substances by using in-situ deposition technique. Using in-situ deposition technique enables to form a conductive polymer coating on the dielectric elastomeric acrylic film.

Polypyrrole electrodes were applied to prestrained dielectric films to construct circular actuators as described earlier. A schematic diagram of preparation of polymerizing pyrrole solution is shown in Figure 32.

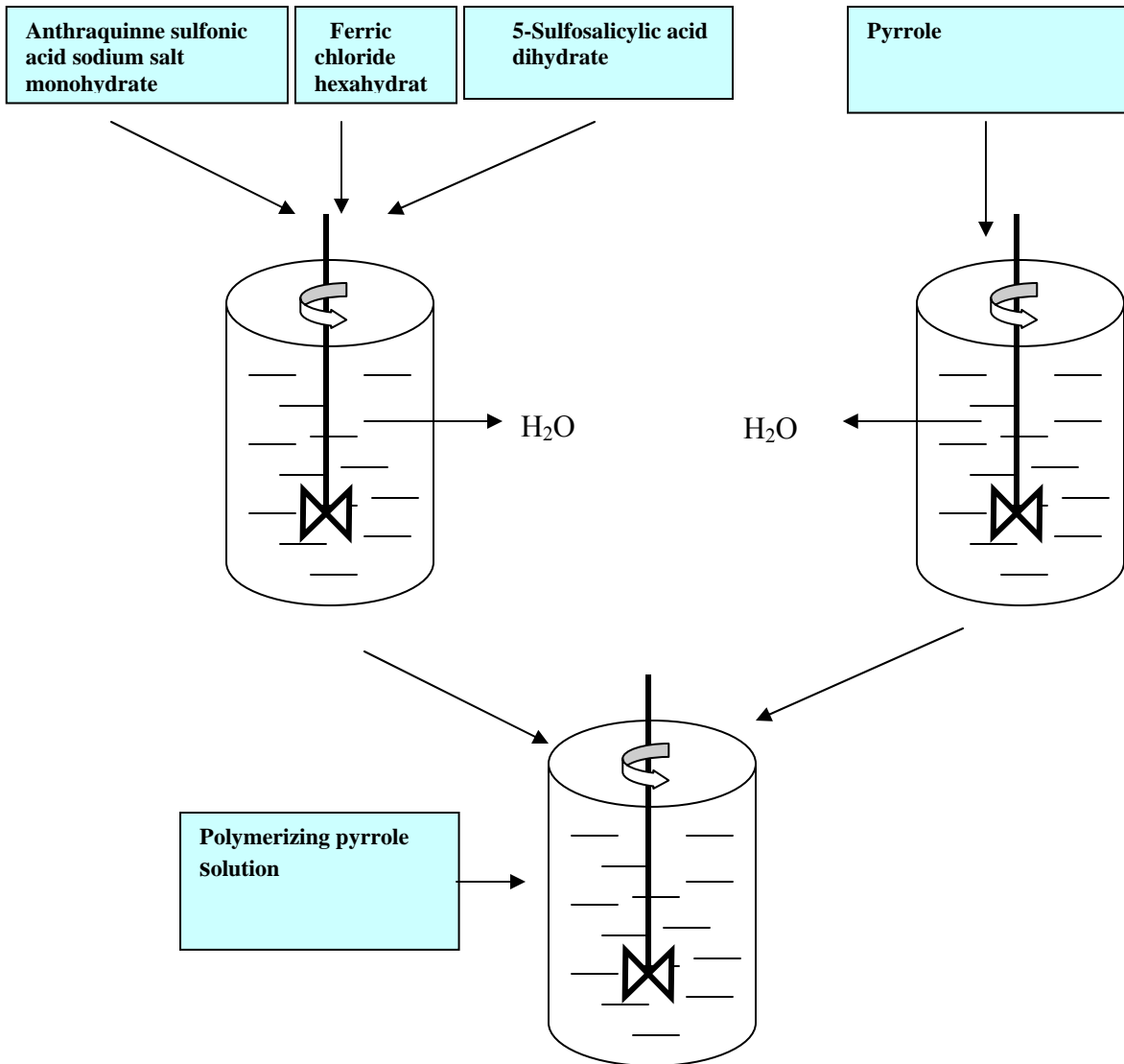


Figure 32: Preparation of polymerizing pyrrole solution

The procedure followed is similar to that described by Su et al [57]. In this process 4.9 g anthraquinone sulfonic acid sodium salt monohydrate, 17.5 g ferric chloride hexahydrate and 26.7 g 5-sulfosalicylic acid dihydrate are dissolved in 500 ml distilled water. In addition 3 ml pyrrole is dissolved in 500 ml distilled water in a separate container. Pyrrole solution is then poured into the other solution and immediately the masked DE actuator film was immersed in this solution.

The process can be carried out under ambient laboratory conditions. Polymerization takes 50 min. In order to obtain polypyrrole electrodes with the desirable quality and thickness, the DE film is removed from the polymerizing solution and is rinsed with distilled water for about 10 sec. Three types of experiments have been carried out for polypyrrole electrodes. One was polymerizing it 3 times. So in this case actuator was removed from the polymerizing solution every 17 min. and rinsed with distilled water. Second was polymerizing it 5 times during the process. So in this case actuator was removed from the polymerizing solution every 10 min. and rinsed with distilled water. The last one was polymerizing it 10 times during the process. In this case actuator was removed from the polymerizing solution every 5min. and rinsed with distilled water. Figure 33 shows the final polypyrrole actuator.



*Figure 33 Polypyrrole coated acrylic film*

### ***4.3 Evaluation of Electrodes***

Three different properties of electrodes were evaluated in this research. These are topography of the electrodes, conductivity of electrodes as a function of applied strain and actuation strain as a function of applied voltage.

#### ***4.3.1 Topography of the Electrodes***

Uniformity and mechanical stability are two important properties of the electrodes in order to achieve the required performance from the final actuator.

Microscopic images were taken in order to evaluate the topography of the electrodes. An optical microscope, Olympus BX 60 with PAX-it-M1243 Modulator 20 X software, was used in order to take the microscopic images of the electrodes, see Figure 34.



*Figure 34:Olympus BX 60*

#### *4.3.2 Electrical Conductivity*

Electrical conductivity is a measure of how well a material accommodates the transport of electric charge. Conductivity may be measured by applying an electrical current to two electrodes and measuring the resulting voltage. A Sony/Tektronik 370 programmable curve tracer equipment was used in order to measure the conductivity of the electrodes in this research. This equipment is a high-performance, GPIB-programmable digital-store curve tracer. The collector supply produces rectified ac or dc voltages ranging from 0 to +/- 2000 volts. Figure 35 shows the picture of this equipment.



*Figure 35: Sony/Tektronik 370 Programmable Curve Tracer*

Two-probe method was used in order to measure the conductivity. In a traditional two-probe method, a current is applied between the probes and the resulting voltage is measured. Gold probes, set at various distances apart, were used for the experiments. The distance between the probes was 0.1", 0.3", 0.5", 0.7" and 0.9".

The samples for the conductivity measurements were prepared on 3M VHB™ 4910 acrylic film, pre-stretched at 250% X 250% nominally in the XY directions as described in section 4.2. A glass slide was attached to the film from the back, the slide together with the film were removed by carefully cutting the film around the slide. Since 3M VHB™ 4910 acrylic film is very sticky, it was easily attached to the glass slide and thus held the pre-strain in the film. Subsequently, the pre-strained film on the glass slide was masked with a plastic film such that a rectangular region was left for the application of electrodes. The

mask was removed after application of electrodes. The process of electrode application of electrode on the pre-strained films has already been described in sections 4.2.1.1, 4.2.1.2 and 4.2.1.3.

The experimental set-up to measure the conductivity of the electrodes under given strain is shown in Figure 36. The set-up, consisted of a microscope platform and an L shaped arm with the probes attached to the end.

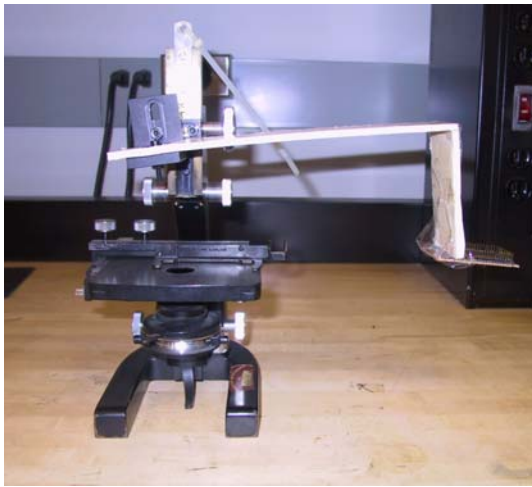


*Figure 36: Microscope platform with arm and plastic plate*

The connection between the probes and the 370 Programmable Curve Tracer equipment was provided with alligator clamps.

Samples for measurement were put on a lab-jack and when the lab-jack was raised, samples with electrodes came into contact with probes and conductivity was measured.

Conductivity of the electrodes was measured from five different spots as shown in Figure 37.

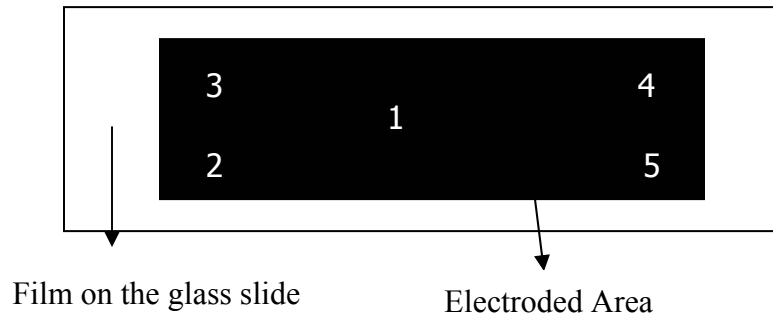


*Figure 37: Conductivity measurement spots for electrodes*

#### 4.3.2.1 Effect of Strain

One of the most important limitations of a DE actuator is the loss of conductivity of the electrodes under strain. An ideal conformable electrode should allow actuation up to dielectric failure of the actuator. Therefore, in order to characterize the performance of a compliant electrode, conductivity as a function of strain is important.

The evaluation of conductivity under strain was done on rubber and PPy electrodes. The samples for the conductivity measurements under strain were prepared on 3M VHB™ 4910 double-coated acrylic foam tape. The VHB film was masked with a plastic film (polyurethane) such that a rectangular region was open for the application of electrodes. Electrodes were applied to the films as per the processes described in sections 4.2.1.1 and 4.2.1.2. After applying the electrode, the film was clamped and stretched on a rigid aluminum frame, see Figure 38.

The experimental set up described earlier in section 4.3.2. Conductivity of the electrodes were measured at four different levels of uniform X-Y strain (0, 50 and 100%).

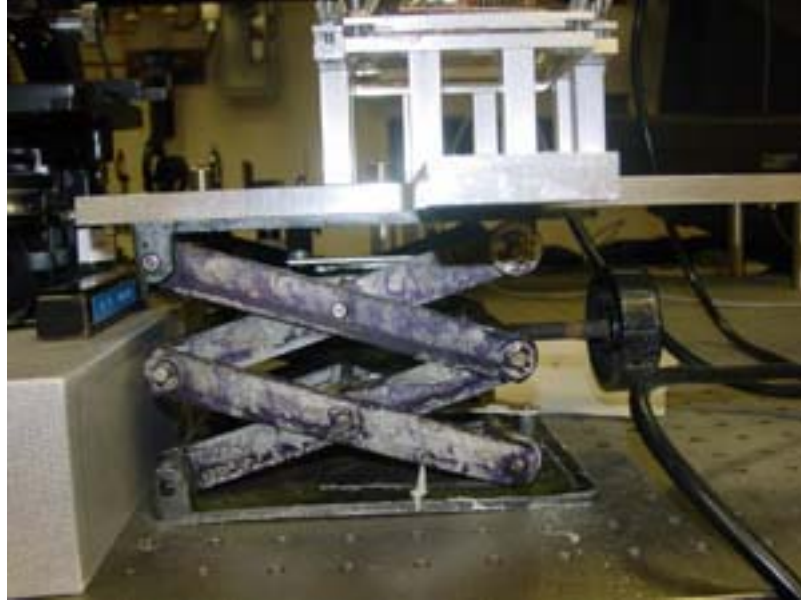


*Figure 38: Frame on the lab-jack*

### *4.3.3 Actuation Strain as a Function of Applied Voltage*

As mentioned earlier, all of the electrode types being investigated were applied to circular DE films (VHB 4910) under 250% x 250% nominal strain. A DC power supply (Gamma) was used as a voltage supplier for all the actuators. The connection between the actuator and the power supply was provided with brass shim and appropriate alligator clamps. The experimental set up is shown in Figure 44 and 45.

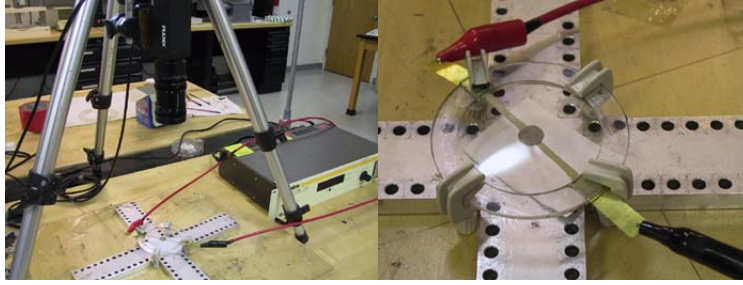


*Figure 39: PPy actuator (connected to the voltage supplier with alligator clamps)*

Voltage was applied from 1kV to 6 kV. During actuation, video images were captured using a camera (TM-9701 Pulnix) controlled by a computer with an image capture card (IMAQ PCI-1407) and LabVIEW image acquisition software. The camera was fitted with a wide-angle lens (Computar H6Z0812). The strain values were calculated from the captured video images using a software (Matrox Inspector 2.1) capable of measuring dimensions accurately.

## 5 Results and Discussion

### *5.1 Topography of the Electrodes*

#### *5.1.1 Nusil CF19-2186 Grease and Rubber Electrodes*

The first experiments were carried out with Nusil CF19-2186 as the polymer carrier. Nusil CF19-2186 is a two-component silicone elastomer manufactured by Nusil Silicone Technology. Grease electrodes were prepared with various levels of graphite by volume (5, 7, 10 and 20%). The procedure used for preparation and application of these electrodes is described in Section 4.2.1.2. For the 5% and 7% mixtures, gel formation was observed immediately after ultra-sound. As a result, it was not possible to use the 5% and 7% mixtures as electrodes.

As described in section 4.2.1.2 during the preparation process of grease electrodes, graphite with heptane and silicone with heptane were poured into a container and this mixture is subjected to the ultra sound for 10 hours. In order to understand the reason for the gel formation, only silicone with heptane was subjected to the ultra sound without graphite and in about 2 hours, gel formation was observed in the two-component silicone because of cross-linking. This experiment showed that gel formation was not related with the presence of graphite in the mixture and might be related with the chemical structure of silicone.

There was no problem of gel formation in preparing mixtures for electrodes with at 10 and 20% graphite content. But crack formation was observed when the electrodes were applied. Figures 40 a and b show the 10 and 20% electrodes on the DE film.

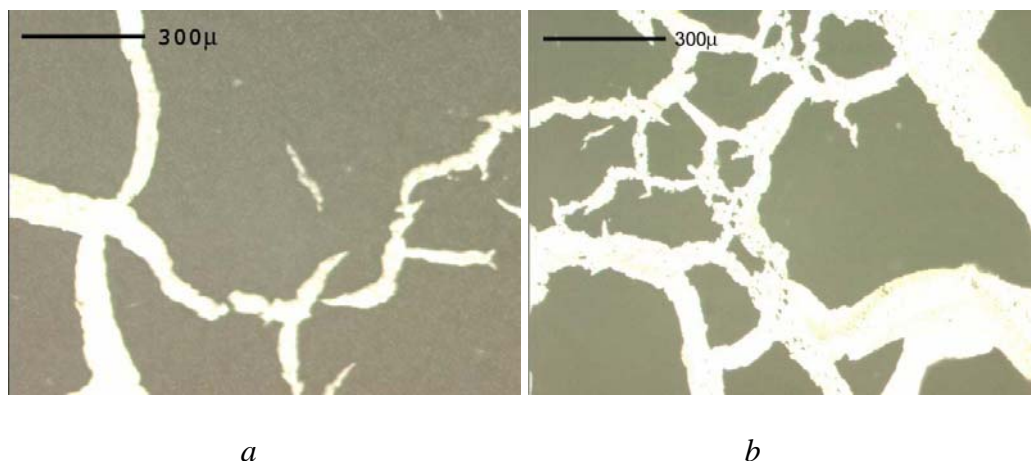
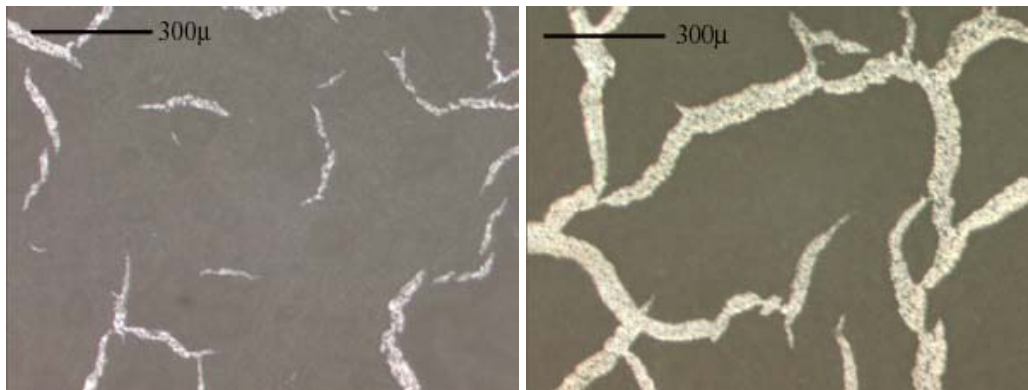


*Figure 40: Nusil CF19-2186 grease electrode a) 10% graphite b) 20% graphite*

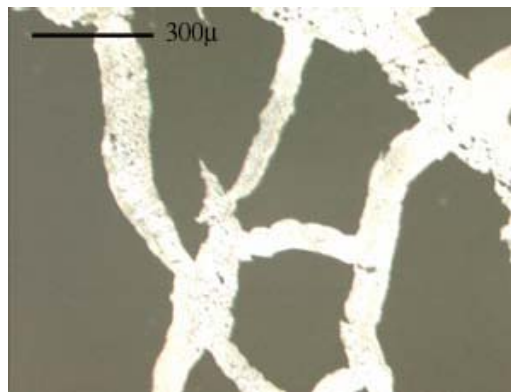
Rubber electrodes were prepared with Nusil CF19-2186. Once again effort was made to prepare rubber electrodes with 2, 5, 10 and 20% graphite content (by volume). It was very difficult to apply the 2% graphite contained electrode on to the DE film as a thin layer. Another problem with the 2% electrodes was storage. Contrary to Kofod's [53] claim the silicone (with 2%graphite) cross-linked in the mixture and gel formation was observed after one week.

The other electrode mixtures showed different characteristics. The 5% graphite contained electrode mixture could be applied to the DE film, but some crack formation was observed, see Figure 41 a. The storage problem described for 2% graphite contained solution was observed for 5% graphite contained electrode mixture also.



*a*

*b*



*c*

*Figure 41: NUSIL CF19-2186 rubber electrode a) 5% graphite b) 10% graphite c) 20% graphite*

It was possible to apply both 10 and 20% graphite contained electrode solutions on to the DE films, but crack formation was found for 20% graphite content compared to 10% graphite content, see Figures 41 b and c.

### 5.1.2 Sylgard 184 Grease and Rubber Electrodes

Another silicone (Sylgard 184) was used as the polymer carrier for both grease and rubber electrodes.

For grease electrodes 5, 10 and 20% graphite content (by volume) electrode mixtures were prepared. It was impossible to smear the 20% graphite contained mixture to the DE film as a thin layer. This was also reported by Kofod [53]. Other two mixtures containing 5 and 10% graphite could be applied to DE films as electrodes. The 5% graphite contained electrode seems to be more uniform. Crack formation was observed with 10% graphite contained electrode. Figure 44 a and b show the taken microscopic images of 5% and 10% electrode mixtures on the DE film.

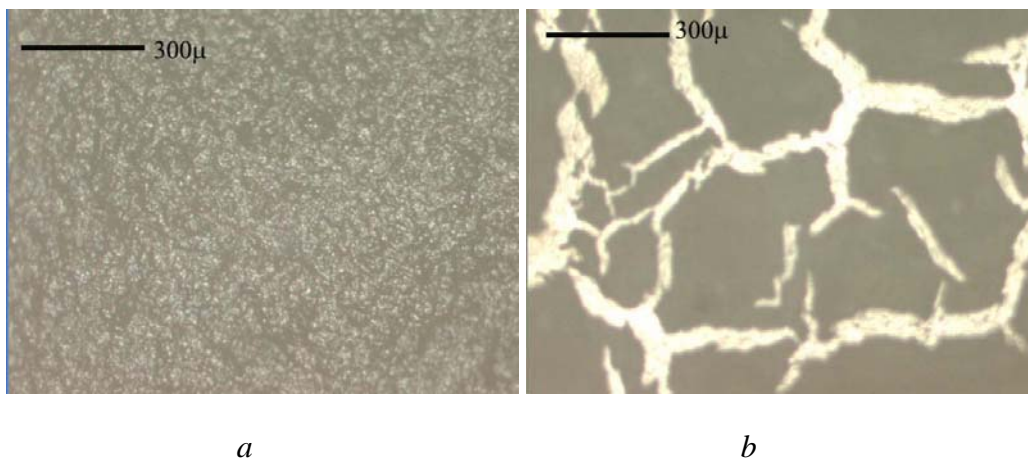
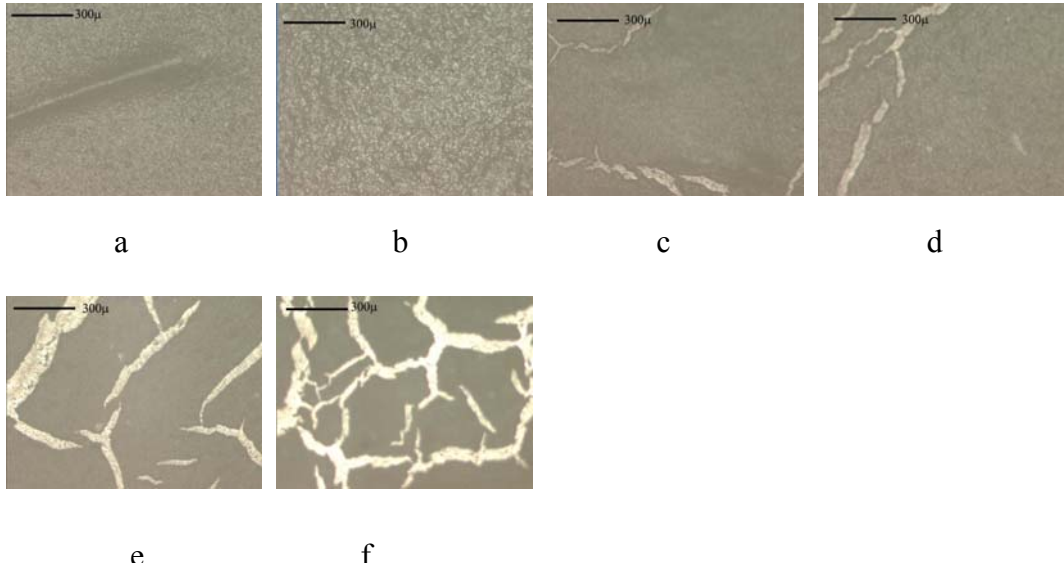


Figure 42: Sylgard 184- Fluid 200® FL 50 CST grease electrode a) 5% graphite b) 10% graphite

In order to understand the reason for the crack formation in the 10% graphite contained electrode further investigations were carried out with electrodes with intermediate levels (6, 7, 8 and 9%) of graphite content. Typical representative images of these electrodes are presented in Figure 43.



*Figure 43: Sylgard 184- Fluid 200@ FL 50 CST grease electrodes a) 5% graphite b) 6% graphite c) 7% graphite d) 8% graphite e) 9% graphite f) 10% graphite*

As seen from the microscopic images, the crack formation starts slightly at 6% level and gradually increases, and reaches to its highest at 10% graphite content. The evidence suggests that a critical level of polymer carrier content is necessary for continuity to form the matrix for the graphite particles.

Rubber electrodes were prepared with Sylgard 184 silicone as the carrier polymer using 5, 10 and 20% graphite content (by volume). All the three electrode mixtures were applied onto the DE films without any difficulty. No crack formation was observed with 5% graphite contained electrodes, see Figure 44 a. Crack formation was observed both with 10

and 20% graphite contained electrodes. Relatively higher level of crack formation was observed with the 20% electrode in comparison to 10% electrode, see Figures 44 b and c .

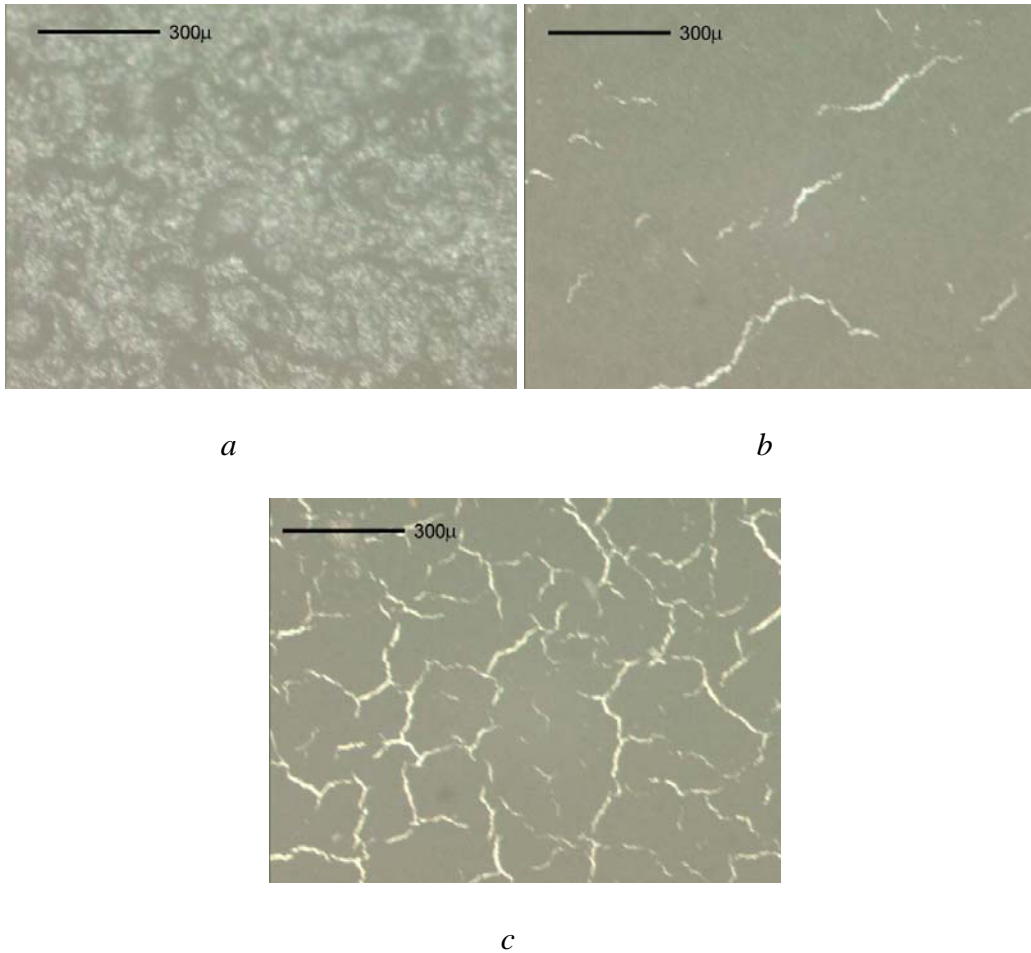


*Figure 44: Sylgard 184- Fluid 200@ FL 50 CST rubber electrode a) 5% graphite b) 10% graphite c) 20% graphite*

### ***5.1.3 Sylgard 186 Grease and Rubber Electrodes***

Sylgard 186 silicone rubber was also used as polymer carrier in order to prepare grease and rubber mixtures. The difference between Sylgard 184 and 186 is their viscosity

and specific gravity values. As mentioned before Sylgard 184 and 186 are two component silicone elastomers. For Sylgard 186 silicone elastomer base the viscosity value is 120000 cSt and for Sylgard 186 silicone elastomer curing agent the viscosity value is 1200 cSt. On the other hand, for Sylgard 184 silicone elastomer base the viscosity value is 5000 cSt and for sylgard 184 silicone elastomer curing agent the viscosity value is 110cSt.

Another difference is their specific gravity values. For Sylgard 186 silicone elastomer base the specific gravity value at 25<sup>0</sup>C is 1.11 and for Sylgard 186 silicone elastomer curing agent the specific gravity value at 25<sup>0</sup>C is 0.98. For Sylgard 184 silicone elastomer base the specific gravity value at 25<sup>0</sup>C is 1.05 and for Sylgard 184 silicone elastomer curing agent the specific gravity value at 25<sup>0</sup>C is 1.03.

To prepare grease electrodes three levels of graphite content (5, 10 and 20%) were chosen. All of these electrode mixtures could be applied without any difficulty. Crack formation was observed with 20% graphite contained electrodes. For other two, no crack formation was observed, see Figure 45 a, b and c.

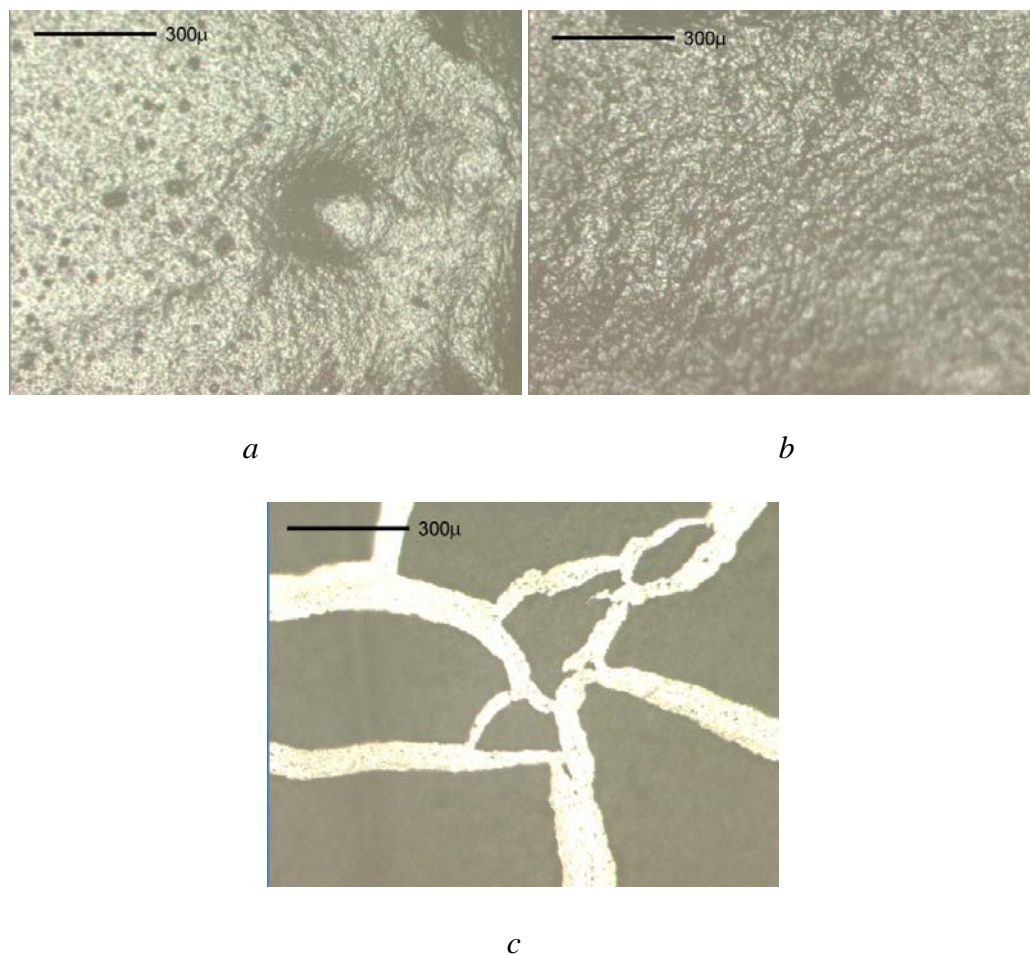
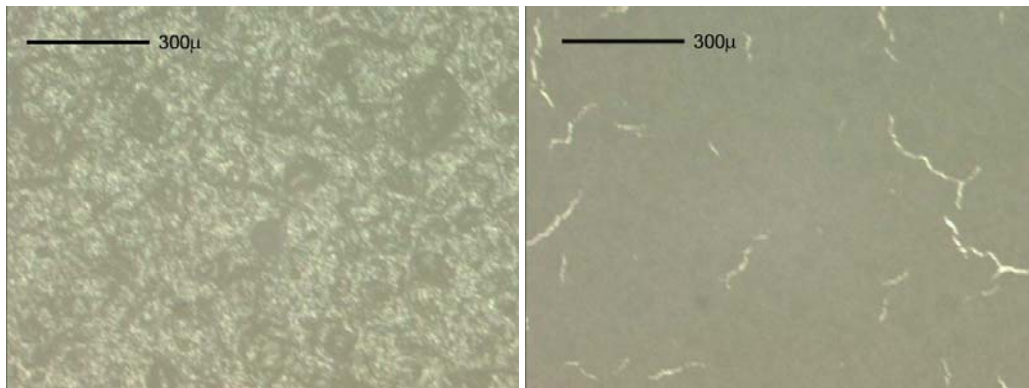


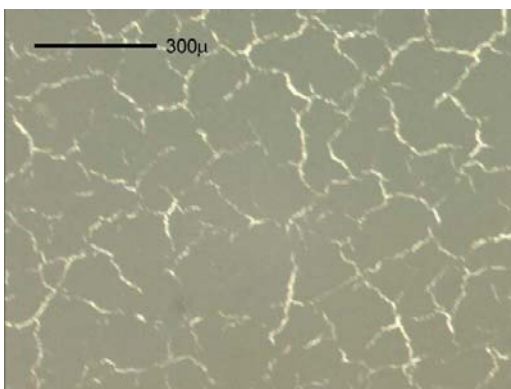
*Figure 45: Sylgard 186- Fluid 200® FL 50 CST grease electrode a) 5% graphite b) 10% graphite c) 20% graphite*

Rubber electrodes were also prepared with Sylgard 186 silicone at 5, 10 and 20% graphite content levels. All the three electrode solutions were applied onto DE films without any difficulty. No crack formation was observed with 5% graphite contained electrodes, see Figure 46 a. Crack formation was observed both with 10% and 20% electrodes. More crack formation was observed with the 20% electrode comparison to 10% electrode, see Figure 46 b and c.



*a*

*b*

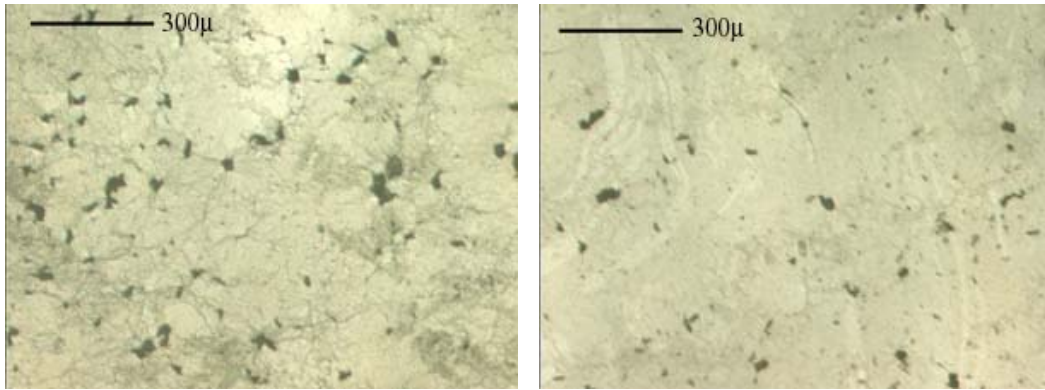


*c*

*Figure 46: Sylgard 186- Fluid 200® FL 50 CST rubber electrode a) 5% graphite b) 10% graphite c) 20% graphite*

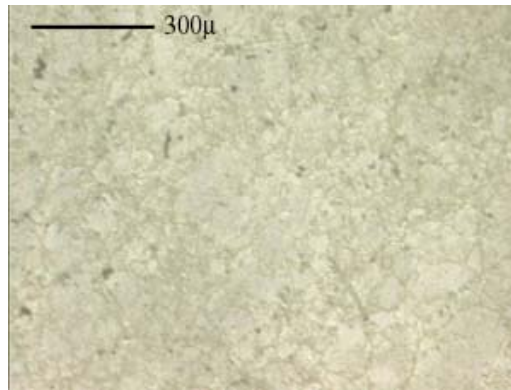
#### ***5.1.4 PPy Electrodes***

In evaluating the topography of polypyrrole conductive polymer electrodes, three types of samples containing three different polymerizing layers (3, 5 and 10 see section 4.2.1.3) were prepared. The micrographs are presented in Figure 47 a, b and c.



*a*

*b*



*c*

*Figure 47: PPy electrode a) polymerized 3 times b) polymerized 5 times c) polymerized 10 times*

It was observed that increasing the number of polymerizing process, thus number of rinsing; enable to remove black polypyrrole particles more efficiently.

## ***5.2 Conductivity of Electrodes***

Conductivity measurements were carried out on all of the electrode samples described thus far. Two-probe method was used in order to measure the conductivity of the electrodes. Since the precise cross-sectional areas of the electrodes could not be obtained easily, the resistance of the electrodes was used to compare the effectiveness of the electrodes. Gold probes were used for the experiments. The distance between the probes was 0.1", 0.3", 0.5", 0.7" and 0.9".

### ***5.2.1 Sylgard 184 Rubber Electrodes***

Figure 48 shows the measured resistance values of the 5, 10 and 20% graphite contained electrodes using Sylgard 184 silicone as a function of probe distance. Figure 49 shows the comparison of the resistance of electrodes. In all of the studies, resistance was measured instead of conductivity. The error bar in the plots indicate 95% confidence interval in all cases.

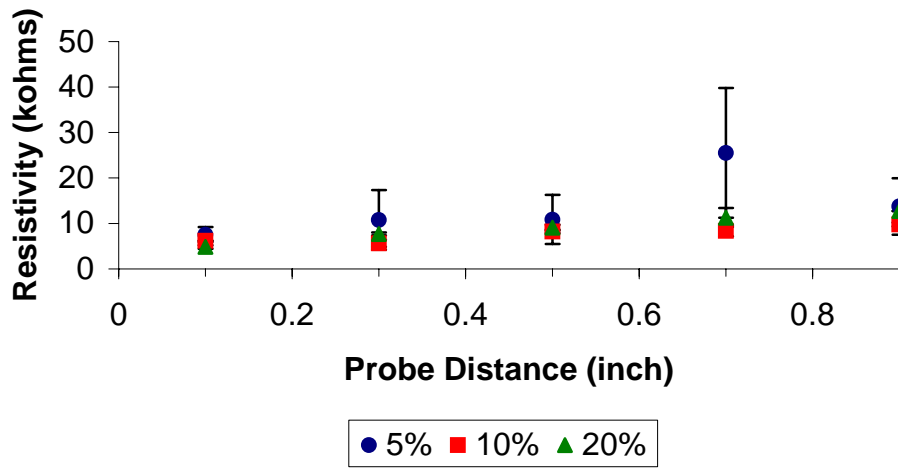


*Figure 48: Resistance values of 5, 10 and 20% Sylgard 184 rubber electrode as a function of distance between the probes*

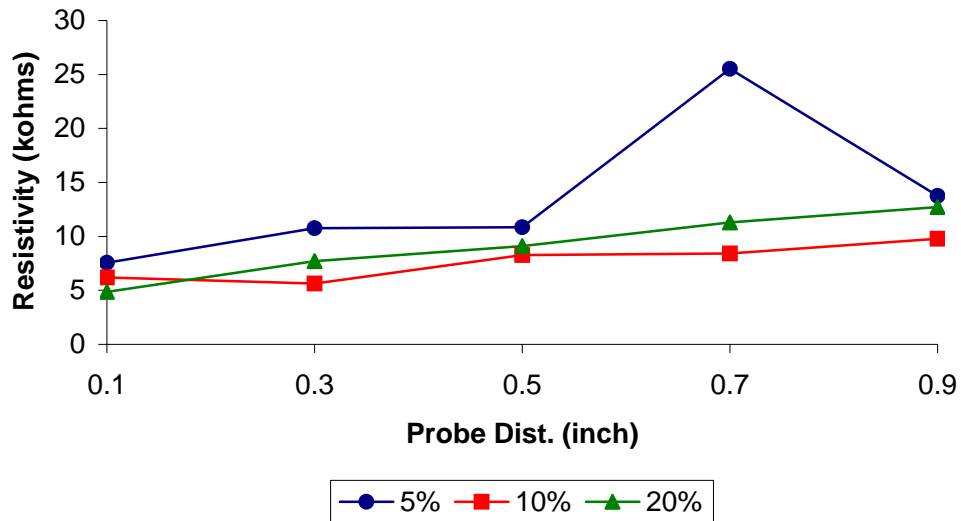


Figure 49: Comparison of the resistance values of the 5, 10 and 20% Sylgard 184 rubber electrodes

As expected resistance values go up with higher probe distance. Comparatively lower resistance was recorded for 10 and 20% graphite contained electrodes for all probe settings. The difference between these two may not be statistically significant, suggesting a percolation threshold around 10%.

### 5.2.2 Sylgard 186 Rubber Electrodes

Figure 50 shows the measured resistance values of the 5, 10 and 20% graphite contained electrodes with Sylgard 186 silicone as the polymer carrier. Figure 51 shows the comparison of the resistance values of all of these electrodes.

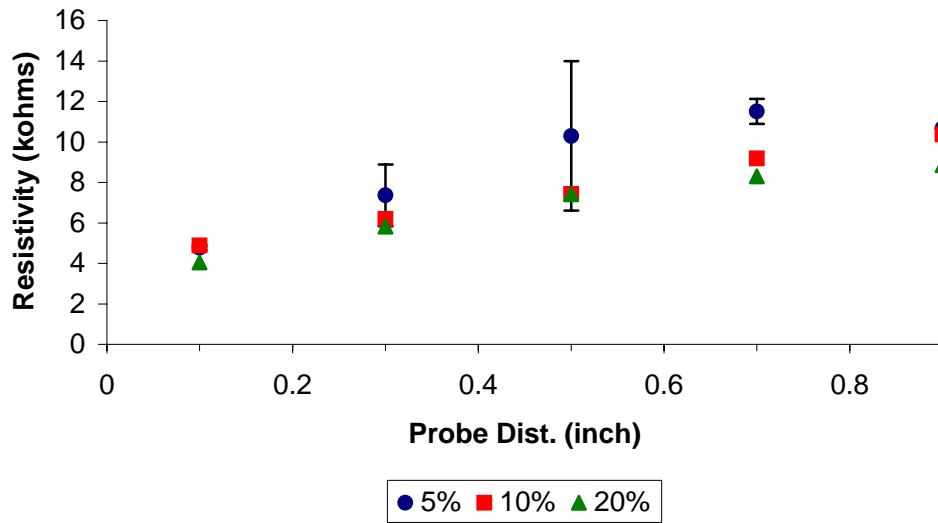


Figure 50: Resistance values of 5, 10 and 20% Sylgard 186 rubber electrode as a function of distance between the probes

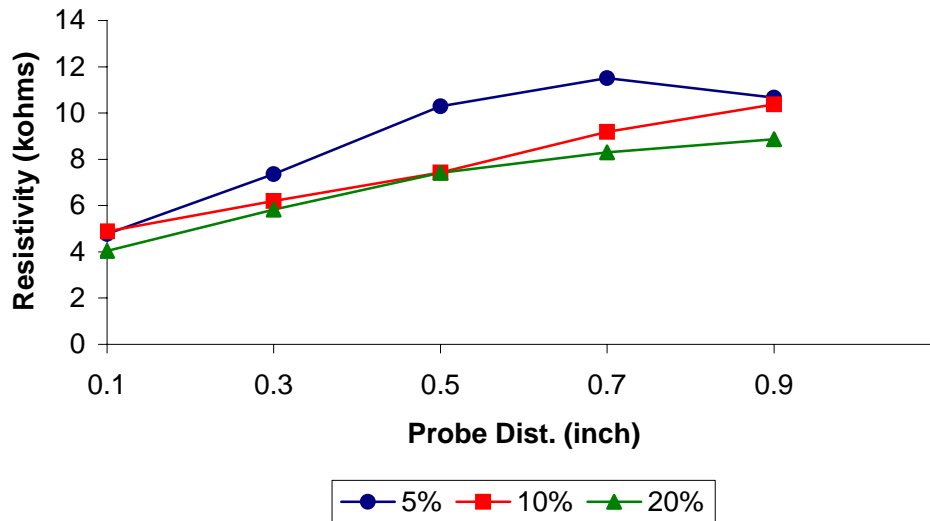


Figure 51: Comparison of the resistance values of the 5, 10 and 20% Sylgard 186 rubber electrodes

The measured values of resistance are similar to that observed for sylgard 184 rubber electrodes. Highest resistance values were observed with the 5% graphite contained electrodes. The resistance values for 10 and 20% electrodes are comparable.

### 5.2.3 Sylgard 184 Grease Electrodes

Conductivity measurements were also carried out on grease electrodes containing 5, and 10% graphite with Sylgard 184 silicone as the polymer carrier, see Figure 52. As mentioned earlier, it was impossible to apply 20% graphite contained Sylgard 184 because of high viscosity.

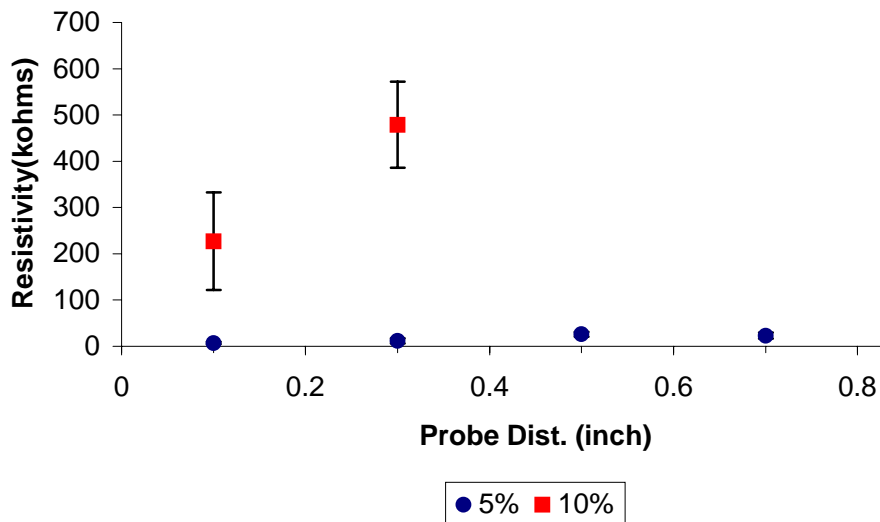


Figure 52: Resistance values of 5 and 10% Sylgard 184 grease electrode as a function of distance between the probes

The electrode containing 10% graphite did not show any measurable conductivity at higher probe distances of 0.5, 0.7 and 0.9 inches. The possible reason is the lack of uniformity and crack formation of the electrode as shown in Figure 42 b.

#### 5.2.4 Sylgard 186 Grease Electrodes

Figure 53 shows the measured resistance values of the 5, 10 and 20% graphite contained Sylgard 186 grease electrodes respectively.

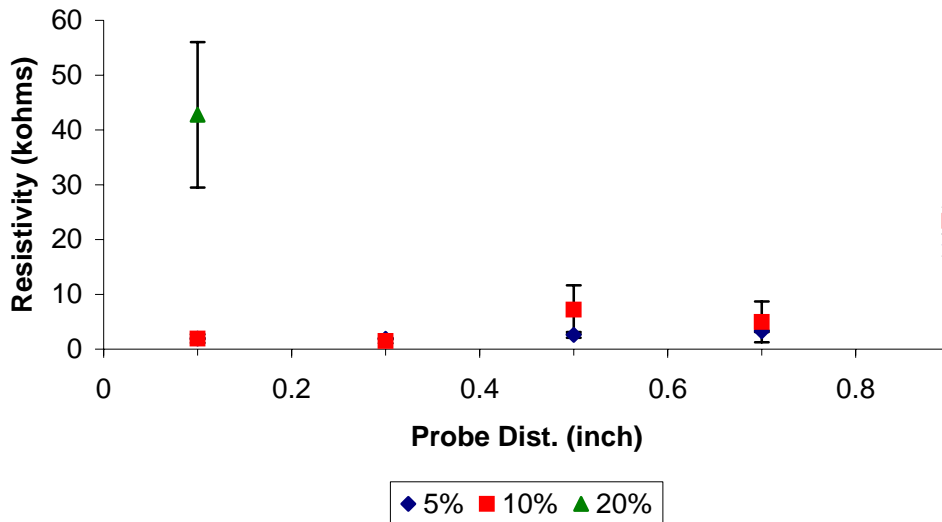


Figure 53: Resistance values of , 5, 10 and 20% Sylgard 186 grease electrode as a function of distance between the probes

The electrode containing 20% graphite did not show any measurable conductivity at probe distances higher than 0.5 inches. Significant level of crack formation was observed at 20% graphite content, see Figure 45 c.

### 5.2.5 PPy Electrodes

Conductivity measurements were also carried out on PPy electrodes containing number of polymerizing layers. Figure 54 shows the measured resistance values of the PPy electrodes, with 3, 5 and 10 polymerizing layers respectively. No significant difference in measured resistance values was observed between these electrodes. Each data point in Figure 54 represents the mean values of 5 measurements together with the confidence interval (95%). The very high level of variability in measured resistance values is a possible indication of high variability in the polymerization of polypyrrole.

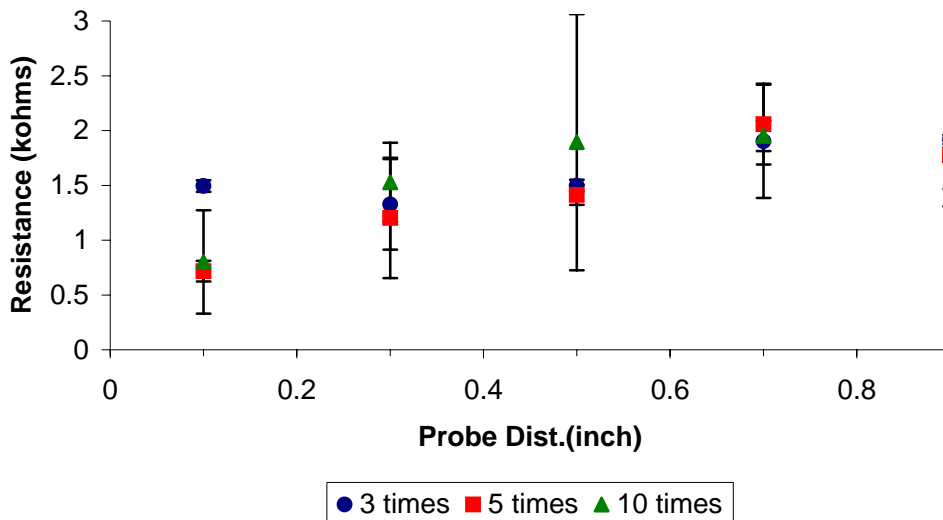


Figure 54: Resistance values of PPy electrode with 3 different polymerizing layers (3, 5 and 10 times) as a function of probe distance

In general, measured grease electrodes seem to have higher resistance values than that of rubber electrodes, but PPy electrodes have the lowest resistance values among the three types of electrodes.

### *5.2.6 Conductivity as a Function of Strain*

As discussed earlier, change of conductivity as a function of applied strain is an important characteristic of electrodes in actuator applications. The methods of preparation of samples for conductivity measurements were described at section 4.4.2. These experiments were carried on rubber and PPy electrodes.

#### 5.2.6.1 PPy Electrodes

The measurement of conductivity under strain was carried out only for PPy electrodes with 5 polymerizing layers. Figure 55 show the resistance values of PPy electrodes under 0%-0% and 50%-50% nominal strain conditions respectively. It should be noted that at strain level of 100%-100%, the resistance was too high to measure. It is obvious that the resistance values increased very significantly at 50%-50% strain compared to zero strain samples. As seen in Figure 56 PPy electrode shows significant cracks under 100%-100%nominal strain conditions.

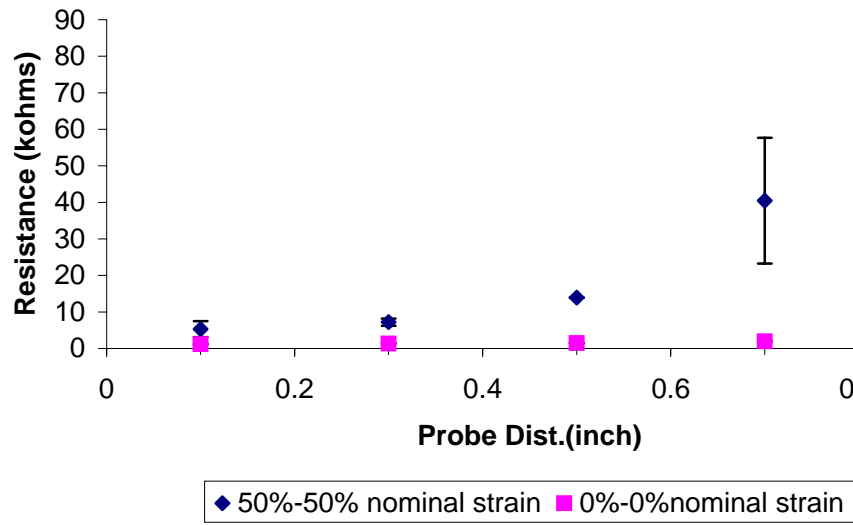


Figure 55: Resistance values of PPy electrode under 0%-0% and 50%-50% nominal strain

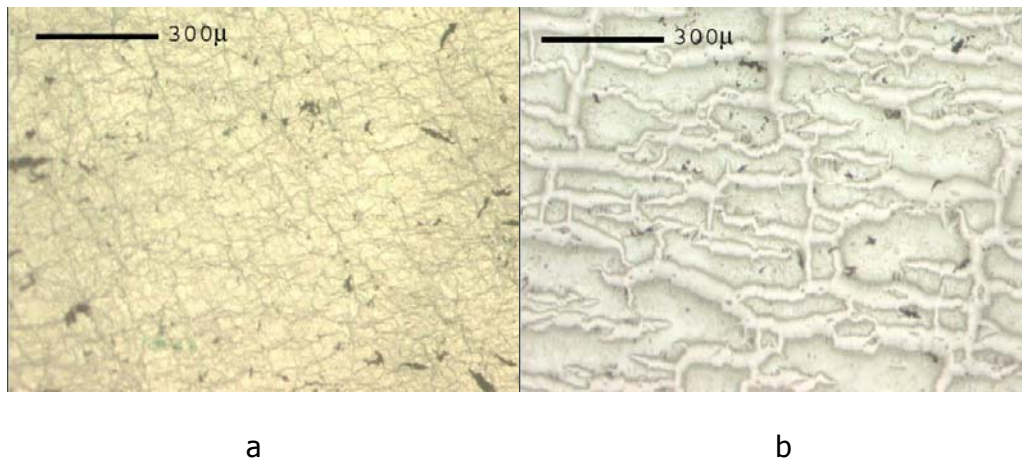
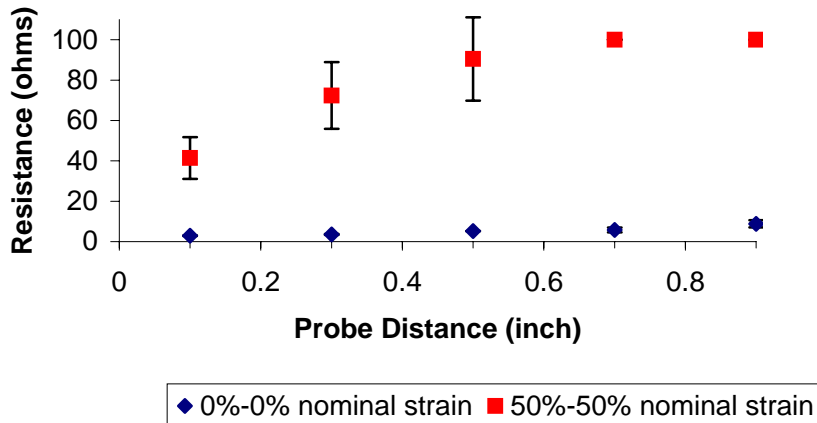


Figure 56: PPy electrode a) under 0%-0% nominal strain b) under 100%-100% nominal strain

### 5.2.6.2 Sylgard 184 Rubber Electrodes

Figures 57 show the measured resistance values of 10% graphite contained electrode using Sylgard 184, under 0%-0% and 50%-50% nominal strain conditions respectively. Similar to PPy electrodes, at 100%-100% strain level, the resistance was too high to measure. Once again, the resistance values are significantly higher at 50%-50% nominal strain. The reasons are somewhat clear from Figures 58 a and b. Crack formation is found significant at 100% strain level.



*Figure 57: Resistance values of Sylgard 184 10% rubber electrode under 0%-0% and 50%-50% nominal strain*

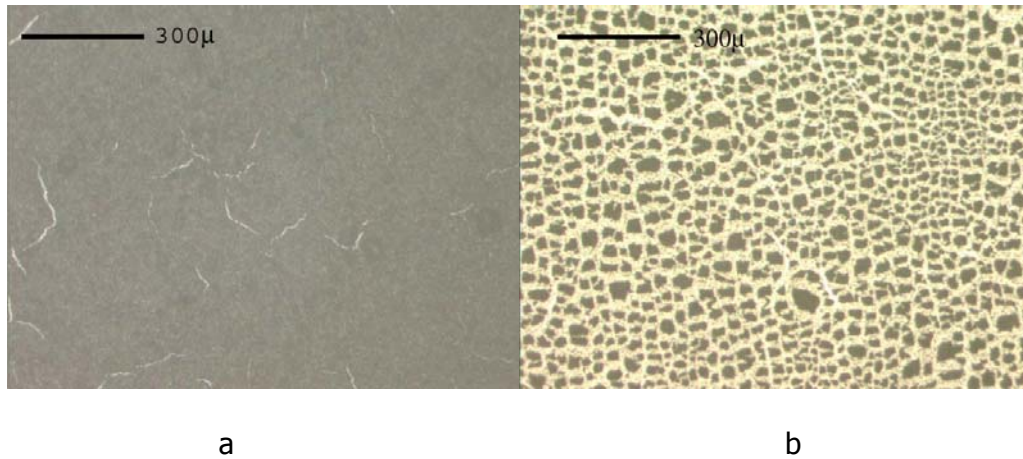


*Figure 58: Sylgard 184 10% rubber electrode a) under 0%-0% nominal strain b) under 100%-100%nominal strain*

#### **5.2.6.3 Sylgard 186 Rubber Electrodes**

Figure 59 shows the measured conductivity values of 10%graphite contained electrode using Sylgard 186, under 0%-0% and 50%-50% nominal strain conditions respectively. Once again, at 100%-100% strain level, the resistance was too high to measure. The measured resistance values are significantly higher at 50%-50% nominal strain. The reasons are somewhat clear from Figures 60 a and b. Crack formation is found significant at 50%strain level.

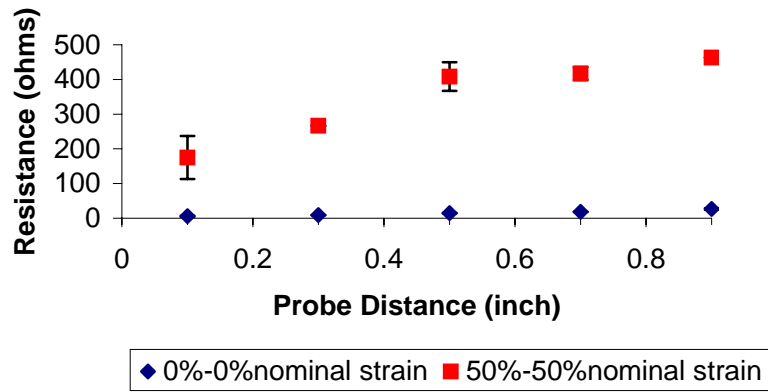


Figure 59: Resistance values of Sylgard 184 10% rubber electrode under 0%-0% and 50%-50% nominal strain

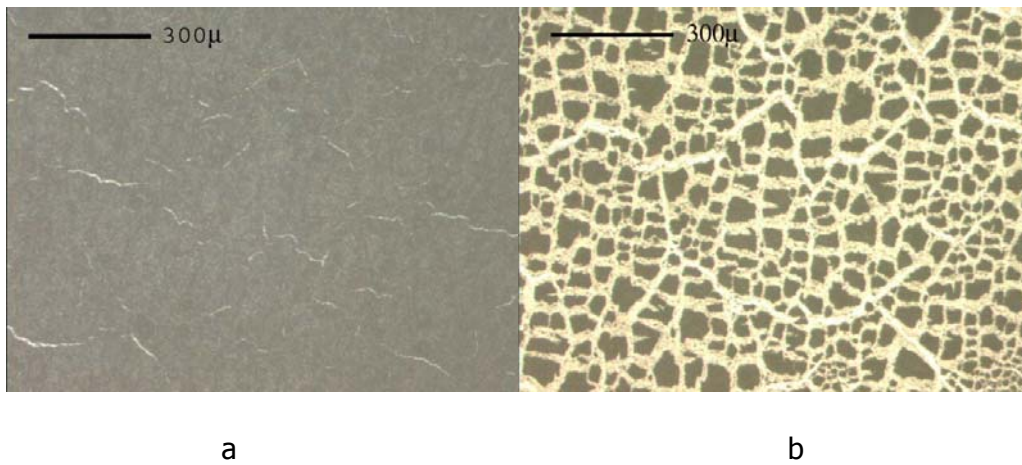


Figure 60: Sylgard 186 10% rubber electrode a) under 0%-0% nominal strain b) under 100%-100% nominal strain

### *5.2.7 Percolation Threshold*

The theory of percolation describes the consequence of varying number of connection in a random network. Percolation in the present context explains how electrons travel through the conductive media. In particle loaded electrode film, Conduction can occur between the particles if the electrons will tunnel and gap jump between conductive particles. This can happen only if the adjacent particles are close enough together, and allow conduction to occur between them.

Kofod [53] explains this using an appropriate example. A box is filled with two types of spherical balls: insulating and conducting. The experiment begins with insulating balls. Conducting balls are then added in random positions one by one while removing insulating balls in order to keep the number of balls constant. At some level, addition of more conducting balls only increase the conductance slightly; therefore a threshold in the conductance becomes distinct. This threshold is called percolation threshold. To determine percolation threshold, experiments have been carried out with Sylgard 184 rubber electrodes at four different levels (3%, 5%, 7% and 10%) of particle content. Electrical resistance values of these electrodes were measured at 0.5" probe distance. Figure 61 shows a plot of the resistance values as a function of particle content. As seen from Figure 61, percolation threshold for graphite-silicone system is at around 7%.

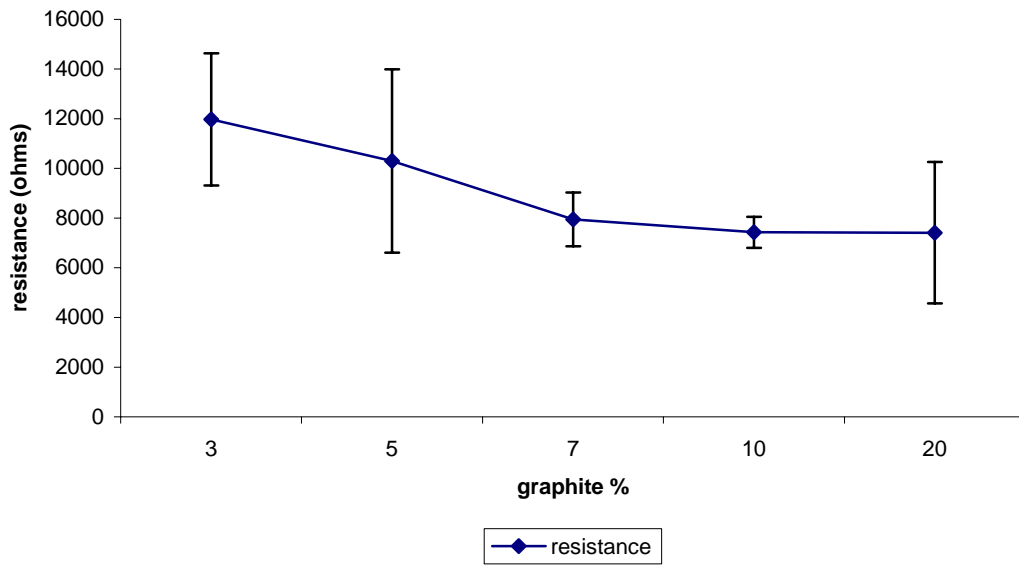


Figure 61: Percolation experiments graph

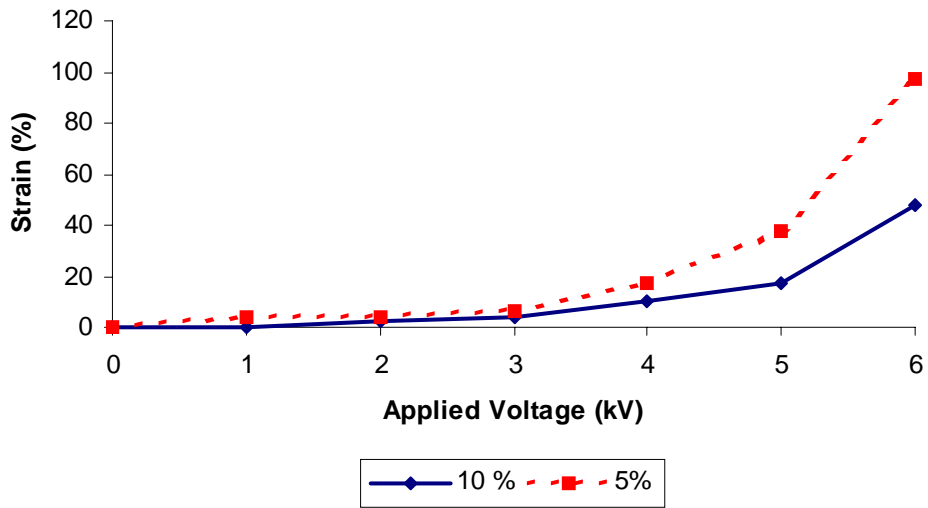
### 5.3 Actuation Strain

One of the important measures of electrode performance in dielectric actuator application is the resulting actuation strain. All of the subject electrodes of this research were evaluated for indicated actuation strain as a function of electrical field. Details of sample preparation as well as actuation strain measurement techniques are described in sections 4.2 and 4.3.3 respectively.

#### 5.3.1 Sylgard 184

Figures 62 and 63 show measured actuation strain for graphite contained Sylgard 184 grease and rubber electrodes as a function of applied voltage. A maximum voltage of 6 kV was applied in all cases. In case of grease electrodes, the 5% graphite contained electrode produced significantly higher level of strain compared to electrodes containing 10% graphite. For 5% graphite loaded Sylgard 184 grease electrode a maximum areal

strain of 97% was observed as opposed to 47% strain for 10% graphite loaded grease electrode. The reasons are somewhat clear from Figure 42. Crack formation was observed for 10% graphite loaded grease electrode.



f

Figure 62: Applied voltage-strain curve for Slygard 184- Fluid 200@ FL 50 CST grease electrodes

The observations for rubber electrodes are somewhat different. In all cases of rubber electrodes the measured actuation strains ranged from 150-160%, see Figure 63.

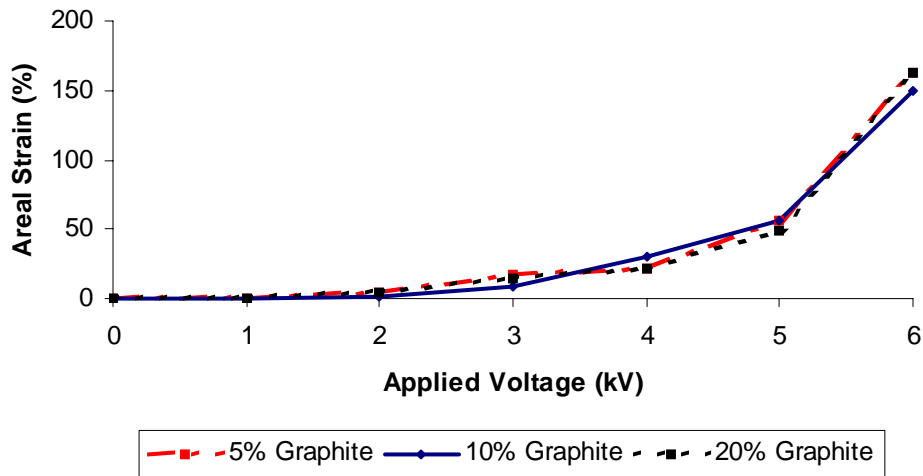


Figure 63: Applied voltage-strain curve for Sylgard 184- Fluid 200@ FL 50 CST rubber electrodes

### 5.3.2 Sylgard 186

In case of grease electrodes, the highest actuation strain of 106% was observed for 10% graphite contained electrodes compared to others, see Figure 64. For 5 and 20% graphite contained electrodes, the maximum actuation strain was measured 87 and 74% respectively.

In case of rubber electrodes, 20% graphite contained electrodes showed the highest level of actuation strain of 96% at maximum voltage. For 5 and 10% graphite contained electrodes the maximum actuation strains of 64 and 69% were observed, see Figure 65.

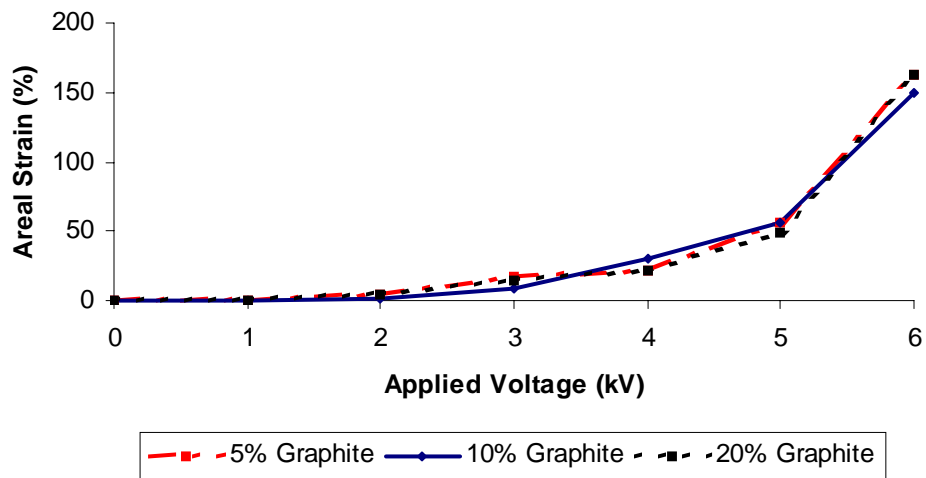


Figure 64: Applied voltage-strain curve for Sylgard 186- Fluid 200® FL 50 CST grease electrodes

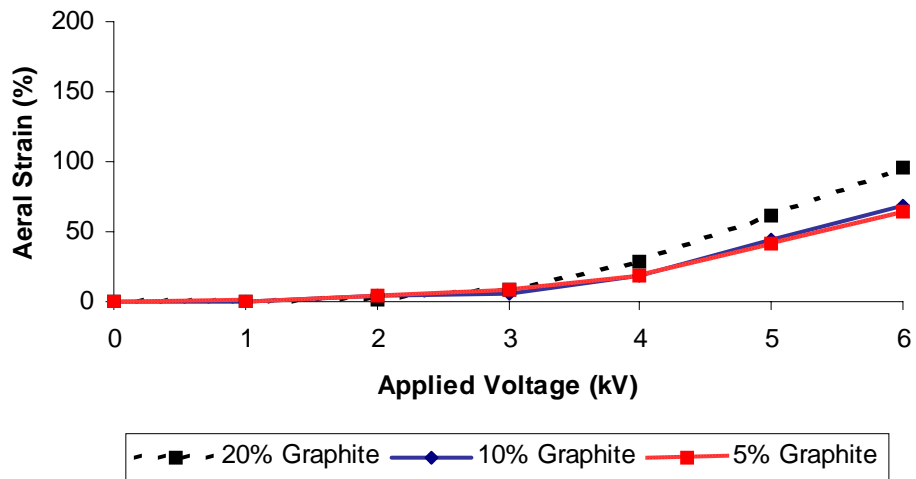


Figure 65: Applied voltage-strain curve for Sylgard 186- Fluid 200® FL 50 CST 5% rubber electrode

It was interesting that 20% electrode gave the highest strain, since it has more crack formation than the other electrodes.

### 5.3.3 PPy Electrodes

As mentioned earlier, 3 types of polypyrrole electrodes with 3,5 and 10 polymerizing layers, were evaluated. There seems to be no significant difference in measured actuation strain for three PPy electrodes. Nevertheless, the highest actuation strain of 17% was observed for the electrode with 5 polymerizing layers. The electrodes with 3 and 10 polymerizing layers showed 11 and 14% maximum actuation strain, see Figure 66.

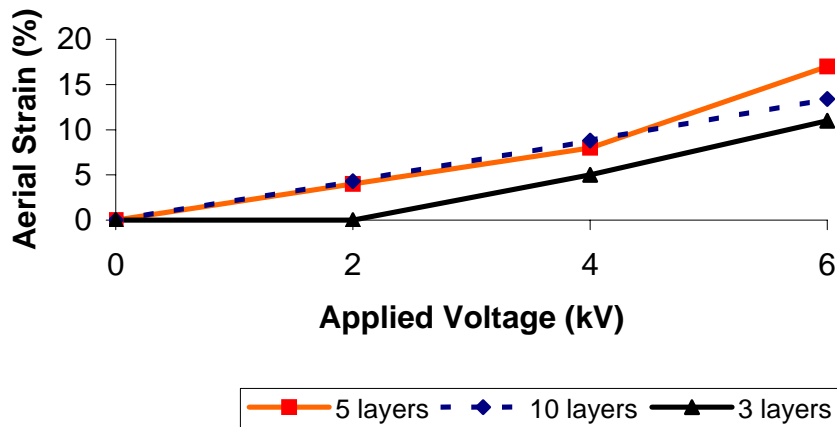


Figure 66: Applied voltage-strain curve for PPy electrode

## 6 Conclusion

Rubber electrodes, grease electrodes and polypyrrole electrodes have been characterized under different process parameters in this research.

Four different types of silicone material were evaluated as polymer carrier for both rubber and grease electrodes. These were; Sylgard®184, Sylgard®186, Nusil CF19-2186 and Fluid 200® FL 50 CST. In order to prepare the electrodes silicone elastomers (Sylgard®184, Sylgard®186) were mixed with Fluid 200® FL 50CST with 50%-50% ratio.

For rubber and grease electrodes, experiments showed that the crack formation was related with the amount of polymer carrier. The amount of crack formation increases when the amount of polymer carrier decreases in the electrode mixture.

Both rubber and grease electrodes, which were prepared with Nusil CF19-2186, showed the worst results in terms of uniformity of the electrodes.

For rubber electrodes, electrodes, which were prepared with Sylgard 186 and Sylgard 184, showed similar results in terms of uniformity of the electrode. No crack formation was observed with 5% electrodes, very slight crack formation was observed with 10% electrodes and higher crack formation was observed with 20% electrodes. Generally Sylgard 184 rubber electrodes showed higher areal strain rates to the applied voltage than that of Sylgard 186 electrodes. Higher conductivity values were achieved with Sylgard 186 rubber electrodes comparing to Sylgard 184 rubber electrodes.

For grease electrodes, electrodes, which were prepared with Sylgard 186 and Sylgard 184 did not show similar uniformity results as rubber electrodes. For Sylgard 184 grease electrodes it was not possible to apply 20% electrode mixture on to the DE film and

10% electrode gave crack formation. No crack formation was observed with 5% electrode.

For Sylgard 186 grease electrodes, it was possible to apply 20% electrode mixture but crack formation was observed. For 5% and 10% electrodes, no problem was observed in terms of crack formation and application of electrodes. Similar areal strain rates were achieved with 5% electrodes both for Sylgard 186 and Sylgard 184 grease electrodes. The areal strain rates were higher for Sylgard 186 10% grease electrodes than that of Sylgard 184 grease electrodes (since crack formation was observed with 10% Sylgard 184 grease electrodes). Higher conductivity values were observed with Sylgard 186 grease electrodes comparing to Sylgard 184 grease electrodes.

Conductivity as a function of strain tests were also carried out for 10% rubber electrodes which were prepared with Sylgard 186 and Sylgard 184. Both Sylgard 184 and Sylgard 186 rubber electrodes lost its conductivity at 100%-100% nominal strain rate even the distance between the probes was 0.1 inch. The reason for this was the uniformity of the electrode under this rate of strain.

Polypyrrole electrodes were also evaluated. There was no significance difference between the electrodes, which was polymerized 3 times, 5 times, and 10 times in terms of uniformity, areal strain and conductivity values. It was observed that increasing the number of polymerizing process, thus number of rinsing, enable to remove black polypyrrole particles more efficiently. Relatively higher conductivity values were achieved with PPy electrodes comparing to rubber and grease electrodes. PPy electrodes lost its conductivity at 100%-100% nominal strain ratio.

## 7 References

1. Cohen Y. B., "Electroactive Polymer (EAP) Actuators as Artificial Muscles", SPIE, Bellingham, Washington, 2001.
2. Wax S.G and Sands R.R (1999) "Electroactive Polymer Actuators and Devices" *Smart Structures and Materials 1999: Electroactive Polymer Actuators and Devices, Proc. SPIE*, Vol. 3669, pp2-9
3. Hanson D., et. al. (2001) "Andoris: application of EAP as artificial muscle to entertainment industry" *Smart Structures and Materials 2001: Electroactive Polymer Actuators and Devices, Proc. SPIE*, Vol. 4329, pp375-379
4. Kornbluh R., et. al. (1999) "High-field electrostriction of elastomeric polymer dielectrics for actuation" *Smart Structures and Materials 1999: Electroactive Polymer Actuators and Devices, Proc. SPIE*, Vol. 3669, pp149-161
5. Cohen Y.B (2002) "Electro-active polymers: current capabilities and challenges" *Smart Structures and Materials 2002: Electroactive Polymer Actuators and Devices, Proc. SPIE*, Vol. 4695, pp1-7
6. <http://www.arch.wustl.edu/538a/thinkingarchit/piezopoly.htm> 12/12/2003

7. Cohen Y. B. and Leary S. (2000) "Electroactive (EAP) Characterization Methods" *Smart Structures and Materials 2000:Electroactive Polymer Actuators and Devices, Proc. SPIE*, Vol. 3987, pp12-16
8. Liu C., et. al. (1999) "Electro-statically stricted polymers(ESSP)" *Smart Structures and Materials 1999:Electroactive Polymer Actuators and Devices, Proc. SPIE*, Vol. 3669, pp186-190
9. Pelrine R., (2002) "Dielectric Elastomer Artificial Muscle Actuators: Toward Biometric Motion" *Smart Structures and Materials 2002: Electroactive Polymer Actuators and Devices, Proc. SPIE*, Vol. 4695, pp126-137
10. Cohen Y. B. (2001) "Transition of EAP material from novelty to practical applications-are we yet" *Smart Structures and Materials 2001: Electroactive Polymer Actuators and Devices, Proc. SPIE*, Vol. 4329, pp1-6.
11. Viewed online at [https://courseware.vt.edu/users/donleo/ME5984/me5984\\_meeting13.pdf](https://courseware.vt.edu/users/donleo/ME5984/me5984_meeting13.pdf) (07/01/2002)
12. Parrot O., et. al. (2001) "Extension Transduction properties of Ionic Polymer Materials" *Smart Structures and Materials 2001:Electroactive Polymer Actuators and Devices, Proc. SPIE*, Vol. 4695, pp228-244

13. Cohen Y., et. al. (2001) "Characterization of the Electromechanical properties of EAP materials" *Smart Structures and Materials 2001: Electroactive Polymer Actuators and Devices, Proc. SPIE*, Vol. 4329, pp319-327
14. Marra S.P., et. al. (1999) "Mechanical properties of active polyacrylonitrile gels" *Smart Structures and Materials 1999: Electroactive Polymer Actuators and Devices, Proc. SPIE*, Vol. 3669, pp226-235
15. Osada Y. and Gong P.J (1999) "Intelligent Gels-Their Dynamism and Functions-" *Smart Structures and Materials 1999: Electroactive Polymer Actuators and Devices, Proc. SPIE*, Vol. 3669, pp12-18
16. Clavert P. and Zengshe L., (1999) "Electrically Stimulated bilayer Hydrogels As Muscles" *Smart Structures and Materials 1999: Electroactive Polymer Actuators and Devices, Proc. SPIE*, Vol. 3669, pp236-241
17. Viewed online at <http://www.azom.com/details.asp?ArticleID=885> (07/12/2003)
18. Kwang J. K. and Shahinpoor M. (1999) "The effect of surface-electrode resistance on actuation of ionic polymer-metal composites (IPMCs)artificial muscles" *Smart Structures and Materials 1999: Electroactive Polymer Actuators and Devices, Proc. SPIE*, Vol. 3669, pp308-319

19. Newbury M. K. and Leo D. J. (2001) "Electrically induced permanent strain in ionic polymer-metal composite actuators" *Smart Structures and Materials 2001:Electroactive Polymer Actuators and Devices, Proc. SPIE*, Vol. 4695, pp67-77
20. Leary S. and Cohen Y. B. (1999) "Electrical Impedance of Ionic Polymeric Metal Composites" *Smart Structures and Materials 1999: Electroactive Polymer Actuators and Devices, Proc. SPIE*, Vol. 3669, pp81-86
21. Madden D.W., et. al. (2002) "Conducting polymer actuators as engineering materials" *Smart Structures and Materials 2002: Electroactive Polymer Actuators and Devices, Proc. SPIE*, Vol. 4695, pp176-190
22. Jager W. H. E. et. al. (1999) "Applications of Polypyrrole Actuators" *Smart Structures and Materials 1999: Electroactive Polymer Actuators and Devices, Proc. SPIE*, Vol. 3669, pp377-384
23. Mak. C.S. and Kosmatka J.B. (2002) "A New Method for Characterizing the Dynamic Properties of Electroviscoelastic Materials" *Smart Structures and Materials 2002: Electroactive Polymer Actuators and Devices, Proc. SPIE*, Vol. 4695, pp277-285
24. Philip N.A., et. al. (2001) "Molecular weight dependence of the physical properties of protonated polyaniline films and fibers" *Smart Structures and Materials 2001:Electroactive Polymer Actuators and Devices, Proc. SPIE*, Vol. 4329, pp475-483

25. Viewed online at <http://physicsweb.org/article/world/11/1/9> (08/09/2003)
26. Mazzoldi A. et. al. (2000) "Electro-mechanical behavior of carbon nanotube sheets in electrochemical actuators" *Smart Structures and Materials 2000:Electroactive Polymer Actuators and Devices, Proc. SPIE*, Vol. 3987, pp25-32
27. Gao M. et. al. (2000) "Electrochemical properties of aligned nanotube arrays: basis of new electromechanical actuators" *Smart Structures and Materials 2000:Electroactive Polymer Actuators and Devices, Proc. SPIE*, Vol. 3987, pp18-24
28. Mavroidis C., et. al. (2000) "Controlled Compliance Haptic Interface Using Electro-rheological Fluids" *Smart Structures and Materials 2000: Electroactive Polymer Actuators and Devices, Proc. SPIE*, Vol. 3987, pp300-310
29. Viewed online at <http://dept.physics.upenn.edu/~kamien/ftp/ftp/ER.pdf> (08/20/2003)
30. Vargha V., et. al. (1999) "Ferroelectric liquid crystal polymers" *Periodica Polytechnica Ser. Cehm. Eng.* Vol. 43, No. 1, pp 17-33
31. Cheng Y., et. al. (2002) "Electromechanical properties and molecular conformation in P(VDF-TrFE) based terpolymer" *Smart Structures and Materials 2002:Electroactive Polymer Actuators and Devices, Proc. SPIE*, Vol. 4695, pp167-175

32. Snyder A., et. al. (2002) "Characterizing electroactive polymers for use in robotic surgical instruments" *Smart Structures and Materials 2002:Electroactive Polymer Actuators and Devices, Proc. SPIE*, Vol. 4695, pp379-386
33. Cheng Y., et. al. (2000) "Characterization of electrostrictive P(VDF-TrFE)copolymers film high frequency and high load applications." *Smart Structures and Materials 2000:Electroactive Polymer Actuators and Devices, Proc. SPIE*, Vol. 3987, pp73-80
34. Chung T.C, et. al. (2001) "Ferroelectric VDF/TrFE/CTFE terpolymers; Synthesis and Electric Properties" *Smart Structures and Materials 2001: Electroactive Polymer Actuators and Devices, Proc. SPIE*, Vol. 4329, pp117-124
35. Kofod G., et. al.. (2001) "Response of dielectric elastomer actuators" *Smart Structures and Materials 2001: Electroactive Polymer Actuators and Devices, Proc. SPIE*, Vol. 4329, pp157-163.
36. Pelrine R., et. al. (2001) "Dielectric Elastomers: Generator Mode Fundamentals and application" *Smart Structures and Materials 2001: Electroactive Polymer Actuators and Devices, Proc. SPIE*, Vol. 4329, pp148-156.
37. Costen C., et. al. (2001) "Model for Bending Actuators That Use Electrostrictive Graft Elastomers " *Smart Structures and Materials 2001:Electroactive Polymer Actuators and Devices, Proc. SPIE*, Vol. 4329, pp436-444

38. Su J., et. al. (2002) "Performance Evaluation of Bending Actuators Made From Electrostrictive Graft Elastomers" *Smart Structures and Materials 2002: Electroactive Polymer Actuators and Devices, Proc. SPIE*, Vol. 4695, pp104-110
39. Kim J., et. al. (2002) "Effects of electrical properties of papers and electrodes for electroactive actuators" *Smart Structures and Materials 2002: Electroactive Polymer Actuators and Devices, Proc. SPIE*, Vol. 4695, pp120-125
40. Kim J., et. al. (2000) "Electro-Active Papers: Its Possibility as Actuators " *Smart Structures and Materials 2000:Electroactive Polymer Actuators and Devices, Proc. SPIE*, Vol. 3987, pp203-209
41. Kim J., et. al. (2001) "Mechanical Performance Improvement of Electro-Active Papers" *Smart Structures and Materials 2001:Electroactive Polymer Actuators and Devices, Proc. SPIE*, Vol. 4329, pp499-504
42. Finkelmann H. and Shahinpoor M. (2002) "Electrically- Controllable Liquid Crystal Elastomer-Graphite Composite Artificial Muscles" *Smart Structures and Materials 2002:Electroactive Polymer Actuators and Devices, Proc. SPIE*, Vol. 4695, pp459-464
43. Shahinpoor M. (2000) "Electrically-activated artificial muscles made with liquid crystal elastomers" *Smart Structures and Materials 2000:Electroactive Polymer Actuators and Devices, Proc. SPIE*, Vol. 3987, pp187-192

44. Kofod G., et. al. (2001) "Actuation response of polyacrylate dielectric elastomers" *Smart Structures and Materials 2001: Electroactive Polymer Actuators and Devices, Proc. SPIE*, Vol. 4329, pp141-147
45. Pelrine R., et. al. (2001) "Applications of dielectric Elastomer Actuators" *Smart Structures and Materials 2001: Electroactive Polymer Actuators and Devices, Proc. SPIE*, Vol. 4329, pp335-349
46. Sommer- Larsen P. et.al (2002). "Performance of dielectric elastomer actuators and materials" *Smart Structures and Materials 2002: Electroactive Polymer Actuators and Devices, Proc. SPIE*, Vol. 4695, pp158-166
47. Choi H. , et. al. (2002) ). "Biomimetic Actuator Based on Dielectric Polymer" *Smart Structures and Materials 2002: Electroactive Polymer Actuators and Devices, Proc. SPIE*, Vol. 4695, pp138-149
48. Kornbluh R. (2000) "Ultrahigh strain response of field-actuated elastomeric polymers" *Smart Structures and Materials 2000: Electroactive Polymer Actuators and Devices, Proc. SPIE*, Vol. 3987, pp51-63
49. Benslimane M., Gravesen P. (2002) "Mechanical properties of Dielectric Elastomer Actuators with smart metallic compliant electrodes" *Smart Structures and Materials 2002: Electroactive Polymer Actuators and Devices, Proc. SPIE*, Vol. 4695, pp150-157

50. Pelrine R., et. al. (2000) "High- Speed Electrically Actuated Elastomers with Strain Greater Than 100% " *Science*, Vol 287, pp 836-839
51. Meijer K., (2001) "Muscle-Like Actuators? A Comparison Between Three Electroactive Polymers" *Smart Structures and Materials 2001: Electroactive Polymer Actuators and Devices, Proc. SPIE*, Vol. 4329, pp7-15
52. Pelrine R., et. al. (2000) "High-field deformation of elastomeric dielectrics for actuators" *Materials Science and Engineering*, C 11, pp 89-100
53. Kofod G., "Dielectric elastomer actuators" The Technical University of Denmark, Ph.D. thesis, September 2001
54. Toth A.L. and Goldenberg A. (2002) "Control System Design for a Dielectric Elastomer Actuator: the Sensory Subsystem" *Smart Structures and Materials 2002:Electroactive Polymer Actuators and Devices, Proc. SPIE*, Vol. 4695, pp323-334
55. Cheng Z.Y., et. al. (1999) "High performance of all electrostrictive systems" *Smart Structures and Materials 1999: Electroactive Polymer Actuators and Devices, Proc. SPIE*, Vol. 3669, pp140-148
56. US patent 5,108,829

57. Su J., et. al. (1998) "Preparation and Characterization of Electrostrictive Polyurethane Films with Conductive Polymer Electrodes" *Polymers for Advanced Technologies*, Vol 9, pp 317-321

58. Watanabe M., et. al. (2002) " Wrinkled Polypyrrole Electrode for Electroactive Polymer Actuators" *Journal of Applied Physics*, Vol 92, number 8, pp 4631-4637.